


Anticipation of food intake induces phosphorylation switch to regulate basolateral amino acid transporter LAT4 (SLC43A2) function

Lalita Oparija¹, Anuradha Rajendran¹, Nadège Poncet¹ and François Verrey^{1,2} 

¹Institute of Physiology and Zurich Center for Integrative Human Physiology (ZIHP), University of Zurich, Zurich, Switzerland

²NCCR Kidney.CH, University of Zurich, Zurich, Switzerland

Edited by: Kim Barrett & Dennis Brown

Key points

- Amino acid absorption requires luminal uptake into and subsequent basolateral efflux out of epithelial cells, with the latter step being critical to regulate the intracellular concentration of the amino acids.
- The basolateral essential neutral amino acid uniporter LAT4 (SLC43A2) has been suggested to drive the net efflux of non-essential and cationic amino acids via parallel amino acid antiporters by recycling some of their substrates; its deletion has been shown to cause defective postnatal growth and death in mice.
- Here we test the regulatory function of LAT4 phosphorylation sites by mimicking their phosphorylated and dephosphorylated states in *Xenopus laevis* oocytes and show that dephosphorylation of S274 and phosphorylation of S297 increase LAT4 membrane localization and function.
- Using new phosphorylation site-specific antibodies, we observe changes in LAT4 phosphorylation in mouse small intestine that correspond to its upregulation at the expected feeding time.
- These results strongly suggest that LAT4 phosphorylation participates in the regulation of transepithelial amino acid absorption.

Abstract The essential amino acid uniporters LAT4 and TAT1 are located at the basolateral side of intestinal and kidney epithelial cells and their transport function has been suggested to control the transepithelial (re)absorption of neutral and possibly also cationic amino acids. Uniporter LAT4 selectively transports the branched chain amino acids leucine, isoleucine and valine, and additionally methionine and phenylalanine. Its deletion leads to a postnatal growth failure and early death in mice. Since LAT4 has been reported to be phosphorylated *in vivo*, we hypothesized that phosphorylation regulates its function. Using *Xenopus laevis* oocytes, we tested the impact

Lalita Oparija is a recent graduate from the University of Zurich, where she obtained a PhD in biology, working in the Epithelial Transport Group of the Institute of Physiology. The data presented in this article were obtained during her PhD and currently she is continuing to investigate these regulatory processes in more detail. Her main scientific interest is the posttranslational regulation of nutrient transporters expressed in the small intestine, and the signalling pathways that control it.



of LAT4 phosphorylation at Ser274 and Ser297 by expressing mutant constructs mimicking phosphorylated and dephosphorylated states. We then investigated the *in vivo* regulation of LAT4 in mouse small intestine using new phosphorylation site-specific antibodies and a time-restricted diet. In *Xenopus* oocytes, mimicking non-phosphorylation of Ser274 led to an increase in affinity and apparent surface membrane localization of LAT4, stimulating its transport activity, while the same mutation of Ser297 decreased LAT4's apparent surface expression and transport rate. In wild-type mice, LAT4 phosphorylation on Ser274 was uniform at the beginning of the inactive phase (ZT0). In contrast, at the beginning of the active phase (ZT12), corresponding to the anticipated feeding time, Ser274 phosphorylation was decreased and restricted to relatively large patches of cells, while Ser297 phosphorylation was increased. We conclude that phosphorylation of small intestinal LAT4 is under food-entrained circadian control, leading presumably to an upregulation of LAT4 function at the anticipated feeding time.

(Received 19 August 2018; accepted after revision 29 October 2018; first published online 31 October 2018)

Corresponding author François Verrey: Institute of Physiology, University of Zürich, Winterthurerstr. 190, CH-8057 Zürich, Switzerland. Email: verrey@access.uzh.ch

Introduction

To contribute to nutrition, proteins need to be properly digested within the intestinal lumen and then absorbed as amino acids and small peptides (Silk *et al.* 1985; Gilbert *et al.* 2008; Nassl *et al.* 2011; Wu, 2016). Amino acids play many central roles, in particular as building blocks for protein synthesis, bioactive molecules, precursors and energy metabolites (Broer, 2008). To reach the cells of other organs and tissues via the bloodstream, amino acids first have to cross the intestinal mucosa, formed by an epithelial layer of enterocytes (Makrides *et al.* 2014). Multiple families of membrane-spanning solute carriers (SLCs) are necessary for proper amino acid transepithelial transport across enterocytes (Palacin *et al.* 1998; Hediger *et al.* 2004; Hundal & Taylor, 2009). First, amino acids are actively transported through the apical brush border membrane into these polarized epithelial cells. This uptake is mainly driven by a co-transport of Na⁺ or H⁺ via symporters or by an exchange with intracellular amino acids via an antiporter (Dave *et al.* 2004; Bohmer *et al.* 2005). The subsequent efflux of amino acids through the basolateral enterocyte membrane appears to be mediated by both antiporters and uniporters. These latter diffusion pathways facilitate efflux of essential amino acids that, to some extent, may recycle back into the enterocytes as exchange substrates of the antiporters. Thereby, uniporters are also necessary for the net efflux of non-essential neutral and cationic amino acids (Rossier *et al.* 1999; Meier *et al.* 2002; Dave *et al.* 2004; Bodoy *et al.* 2005; Ramadan *et al.* 2007; Guetg *et al.* 2015; for reviews see Verrey, 2003; Poncet & Taylor, 2013; Broer & Broer, 2017). It has also been suggested that basolateral uniporters might quantitatively control overall basolateral amino acid efflux (Mariotta *et al.* 2012; Guetg *et al.* 2015; Vilches *et al.* 2018).

In normal physiological conditions, nutrient intake is adjusted to dietary needs and is subject to a

circadian rhythm. This rhythm is hierarchically organized with the suprachiasmatic nucleus (SCN) of the hypothalamus functioning as a master regulator integrating environmental (e.g. light) and internal (e.g. feeding) signals into a functional diurnal regulatory system (Welsh *et al.* 2010; Albrecht, 2012; Balakrishnan *et al.* 2012). Nonetheless, cells in many organs and tissues express multiple clock genes (*Clock*, *Bmal1*, *Per1–2*, *Cry1–2* amongst others) that are transcriptional regulators with ~24 h rhythmicity. The functional output of these peripheral clocks is mediated by so called clock-controlled genes (CCGs) that act as effectors or also as transcriptional regulators. The peripheral clock of intestinal cells has been shown to bypass the SCN-cued rhythm to generate and control its own oscillatory rhythm, with a feeding-fasting pattern being the dominant cue (Mohawk *et al.* 2012; Schibler *et al.* 2015). Experiments performed with rodents have indeed revealed that time-restricted feeding can induce or reset the circadian rhythm of the intestine, in particular regarding its glucose and peptide transport capacity (Stephan *et al.* 1979; Pendergast *et al.* 2009; Konturek *et al.* 2011; Balakrishnan *et al.* 2012; Pacha & Sumova, 2013; Hussain & Pan, 2015).

In contrast to the substantial number of studies on glucose and peptide absorption or transport regulation, research on diurnal regulation of intestinal amino acid transport is scarce. One study has shown that dynamic feeding of the amino acid methionine affects mRNA expression of a number of apical and basolateral transporters in jejunum of laying hens (Yi-lin *et al.* 2017). In addition, in a recent study we have observed that rats during their active/feeding phase (ZT15) display increased apical amino acid symporter B⁰AT1 (SLC6A19) protein expression and B⁰AT1-mediated amino acid uptake rate in proximal jejunum (Jando *et al.* 2017). It has also been shown that amino acid transporters (AATs) can be regulated by their own substrates and that several

hormones such as gastrin, glucagon and insulin might play a role as mediators (William & Diamond, 1983; McGivan & Pastor-Anglada, 1994; Gazzola *et al.* 2001; Havel, 2001; Tanaka *et al.* 2005). These studies indicate that AATs are adaptive to nutritional signals and that diurnal regulation may, on the one hand, mediate changes in amino acid transporter expression that imply relatively short mRNA and/or protein half-lives and, on the other hand, lead to changes in AAT function and/or localization. However, detailed mechanisms and signalling pathways leading to AAT diurnal regulation are largely unknown, especially regarding the possible role of post-translational modifications of transporters.

Proteins can be modified by addition and/or withdrawal of one or several chemical groups, and such post-translational modifications can fine-tune their localization, stability and activity in a fast and dynamic way (Deribe *et al.* 2010). The most common modifications include phosphorylation, glycosylation, lysine acetylation, ubiquitination and proteolytic processing (Venne *et al.* 2014). Protein phosphorylation – the attachment of a phosphate group on serine, threonine or tyrosine residues by protein kinases – has been shown to be a central mechanism for the regulation of several crucial functions such as overall cellular communication, metabolism, proliferation and autophagy (Deribe *et al.* 2010; Karve & Cheema, 2011). Thus it is not surprising, that phosphorylation has been shown to play a role in the regulation of some epithelial AATs, for instance of the neutral and cationic amino acid transporter ATB^{0,+} (SLC6A14) (Samluk *et al.* 2012), of the cystine and dibasic AAT rBAT-b^{0,+}AT (SLC3A1-SLC7A9) (Mizoguchi *et al.* 2001), of the glycine and GABA transporter VIAAT (SLC32A1) (Bedet *et al.* 2000) and of the glutamate transporter EEAC1 (also called EAAT3, SLC1A1). In the case of EEAC1 two subtypes of protein kinase C were shown to increase its cell surface expression and/or activity (Gonzalez *et al.* 2002). In contrast, so far no intestinal basolateral amino acid transporter has been shown to be regulated by phosphorylation, although putative phosphorylation sites have been predicted and detected in (phospho-)proteomic studies for most of them, including LAT1 (SLC7A5), LAT2 (SLC7A8) and TAT1 (SLC16A10) (Hornbeck *et al.* 2015) (<https://www.phosphosite.org>). A well-known example of another basolateral transport protein that is regulated by phosphorylation is Na⁺ K⁺-ATPase. For instance, it is phosphorylated by gastrin-cholecystokinin B-induced signalling, causing its translocation to an endosomal compartment, thus inhibiting sodium transport (Liu *et al.* 2016). Moreover, although phosphorylation would be a good candidate mechanism for AAT regulation in intestinal epithelia during feeding-fasting cycles, to our knowledge no study investigating this relationship has been published yet.

LAT4 (SLC43A2) is a unique basolateral amino acid transporter. It belongs to the system L amino acid transporters meaning that it transports large neutral amino acids in a Na⁺-independent way. Specifically, it is a uniporter transporting only a few essential amino acids, namely phenylalanine, methionine and the branched chain amino acids leucine, isoleucine and valine by facilitated diffusion (Bodoy *et al.* 2005). In the small intestine of mice, the protein expression of LAT4 has been detected in the epithelial cells of the villi and it appears to be absent from the crypts. We have shown that the deletion of LAT4 led to a slight intra-uterine growth retardation, postnatal growth failure and early death (prior to postnatal day 10) in mice; possibly due to defective amino acid (re)absorption. Interestingly, the lack of LAT4 in pups affected the plasma concentration of several amino acids that are not its substrates, indicating a possible gatekeeper function (Guettg *et al.* 2015). Thus, we hypothesized that LAT4 expression, localization or function could be regulated to ensure optimal transepithelial amino acid transport and homeostasis.

Phosphorylation of LAT4 has been detected in numerous (phospho-)proteomic studies, but has never been investigated in detail. The phosphosites identified most often are conserved between human and mouse and the corresponding serine residues are numbered identically: serine274 (S274), serine278 (S278) and serine297 (S297) (for specific references see the PhosphoSitePlus database: (Hornbeck *et al.* 2015) (<https://www.phosphosite.org>)). We therefore hypothesized that LAT4 function could be regulated by phosphorylation and/or dephosphorylation of specific serine residues or combinations thereof.

To investigate the potential role of S274, S278 and S297 phosphorylation in the regulation of LAT4, we created phosphorylation and non-phosphorylation mimicking human LAT4 (hLAT4) mutants, expressed them in *Xenopus laevis* oocytes and assessed the impact of these mutations on hLAT4 subcellular localization and function. To study the potential regulation of mouse LAT4 (mLAT4) by phosphorylation *in vivo*, we tested new, custom-made, affinity-purified phosphorylation site-specific antibodies (Pineda, Berlin, Germany). We used these new antibodies to assess whether a time-restricted diet induces diurnal changes in phosphorylation of small intestine mLAT4 in mice.

Methods

Ethical approval

All experimental procedures and handling involving mice and *Xenopus laevis* frogs were approved by the Cantonal Veterinary Office of Zurich (reference no. ZH075/15 for

mice experiments) and performed in accordance with Swiss Animal Welfare laws. The study was done in compliance with ethical principles and standards of *The Journal of Physiology*.

Animal housing and experimental set-up

To provide negative controls for antibody testing, we created conditional LAT4 knockout mice by breeding tamoxifen-inducible ROSA^{Cre} mice (B6.129-Gt(ROSA)26Sor^{tm1(cre/ERT2)Tyj/J}) (IMSR Cat. No. JAX:008463, RRID:IMSR.JAX:008463, The Jackson Laboratory, Bar Harbor, ME, USA) with custom-made LAT4^{flx/flx} mice (C57Bl/6N background, PolyGene AG, Rumläng, Switzerland) in Laboratory Animal Services Center (LASC) facilities at University of Zurich (conditional LAT4 knockout; *manuscript in preparation, Rajendran, Poncet, Oparija, Verrey*).

Eighteen 8-week-old LAT4^{flx/flx}ROSACreERT^{wt} (further referenced as WT LAT4 mice) and tamoxifen-induced LAT4^{flx/flx}ROSACreERT⁺ mice (further referenced as LAT4 KO mice) of both genders, previously housed in standard laboratory conditions and fed 18% protein diet (Kliba Nafag, Kaiseraugst, Switzerland) *ad libitum*, were transferred to climate chambers with an inverted 12 h dark/light cycle, the dark (active) period starting at 09.00 h (ZT12). The temperature in the climate chambers was kept constant at 22°C. After a 1 week adjustment to the inverted rhythm, restricted feeding was started with chow given from ZT12 to ZT20. All animals had *ad libitum* access to water. After 3 weeks of restricted feeding, mice (weight range: from 17.5 to 32 g) were killed by cervical dislocation either at the start of the active phase after 16 h of starvation (ZT12), or at the start of the passive phase (ZT0) 4 h after chow withdrawal. Harvesting and preparation of small intestinal mucosa was optimized to minimize proteolytic degradation. Duodenal (first 7 cm), jejunal and ileal (last 5 cm) parts of the small intestine were placed into ice-cold PBS 1–2 min after killing and from each part 4 cm (proximal duodenum and ileum, distal jejunum) were everted and scraped on an ice-cold surface to collect mucosal cells. All samples were then snap frozen in liquid nitrogen within 6–7 min of killing. The rest of the small intestine was fixed for immunofluorescence as described in the corresponding section below. Mice were assigned to each time point randomly and later data analysis did not show any significant gender-specific effects on our investigated parameters (data not shown). Killing, organ harvesting and sample processing were done in a blinded manner.

Antibodies

Anti-mouse LAT4 antibody production and specificity testing was performed as previously described (Guett *et al.*

2015). Affinity purified anti-mouse LAT4 phosphoS274 (pS274) and phosphoS297 (pS297) antibodies targeted to the phosphorylation sites in the third intracellular loop (epitopes NH₂-CVGRRL(pS)VGS-CONH₂ and NH₂-CEGHKLSL(pS)TVDLEVK-CONH₂, accordingly) were custom made (rabbit polyclonal) (Pineda, Berlin, Germany). Since hLAT4 constructs were FLAG-tagged, commercially available anti-FLAG antibody (rabbit polyclonal) was used (Sigma-Aldrich Cat. No. F7425, RRID:AB_439687, Sigma-Aldrich, Buchs, Switzerland) for detection of hLAT4 expressed in *Xenopus* oocytes. However, two different lots were used during this study: Lot No. 085M4774V for experiments represented in Fig. 1 and 2; and Lot No. 018M4828V for experiments represented in Fig. 3, with the latter lot showing increased non-specific antibody binding.

To detect β -actin (Sigma-Aldrich Cat. No. A2228, Lot No. 066M4860V, RRID:AB_476697) and β -tubulin (Sigma-Aldrich Cat. No. T8328, Lot No. 113M4769V, RRID:AB_1844090) commercially available mouse monoclonal antibodies were used (both from the distributor Sigma-Aldrich, Buchs, Switzerland). For E-Cadherin detection commercially available rat monoclonal antibody was used (Innovative Research Cat. No. 13–1900, Lot No. SK2474191A, RRID:AB_86571, Invitrogen, Carlsbad, CA, USA). As secondary antibodies for Western blotting (WB) anti-rabbit IgG HRP conjugate (Promega Cat. No. W4011, Lot No. 0000236621, RRID:AB_430833) and anti-mouse IgG (H+L) AP conjugate (Promega Cat. No. S3721, Lot No. 0000261214, RRID:AB_430871) were used (both from the distributor Promega, Dübendorf, Switzerland). For immunofluorescence (IF) Alexa Fluor 594 (Abcam Cat. No. ab96921, Lot No. GR170389-3, RRID:AB_10680407) and 488 (Abcam Cat. No. ab150061, Lot No. GR242534-5, RRID:AB_2571722) donkey anti-rabbit IgG (H+L) (both from distributor Life Technologies, Carlsbad, CA, USA) and Alexa Fluor 488 goat anti-rat IgG (H+L) (Thermo Fisher Scientific Cat. No. A-11006, Lot No. 1887148, RRID:AB_2534074, Invitrogen, Carlsbad, CA, USA) polyclonal antibodies were used. Submembrane actin cytoskeleton staining in *Xenopus laevis* oocytes was done using X-phalloidin Texas Red 594 (Cat. No. T7471, Lot No. 28581W, Invitrogen, Carlsbad, CA, USA). Cell nuclei were detected with 4,6-diamidino-2-phenylindole (DAPI) (Thermo Fisher Scientific Cat. No. D3571, Lot No. 778144, RRID:AB_2307445, Invitrogen, Carlsbad, CA, USA).

Mutagenesis of hLAT4 cDNA and cRNA synthesis

Cloning of hLAT4 into pSDeasy vector and FLAG-tagging the construct was done as described previously (Taslimifar *et al.* 2017). To mutagenize serines 274, 278 and 297 to either alanine (A) or glutamate (E), the QuikChange Lightning Site-Directed mutagenesis kit was used (Cat. No. 210519-5, Lot No. 0006298219, Agilent Technologies,

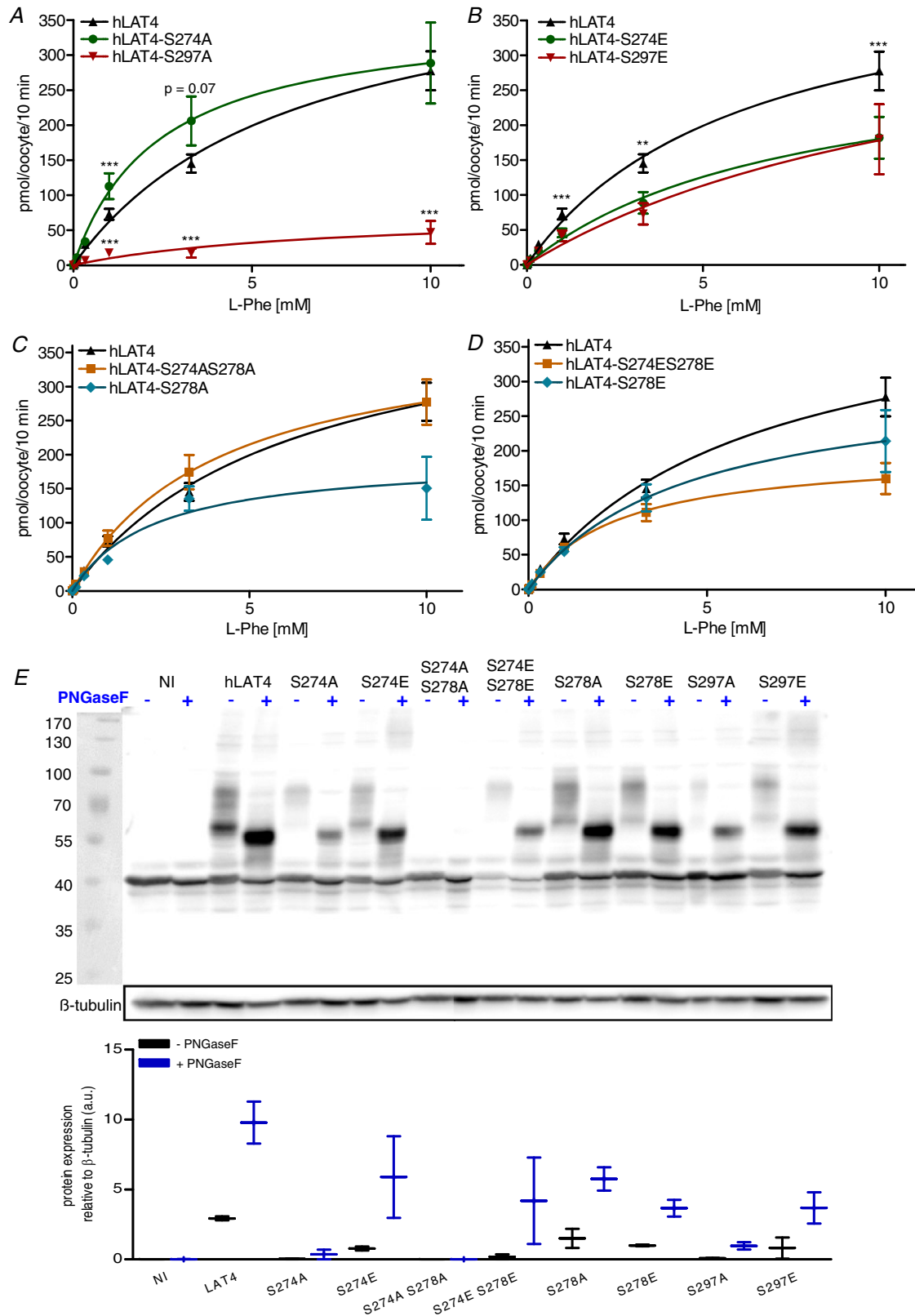


Figure 1. Mimicking dephosphorylation reveals potential regulation of LAT4 expression and function
 A–D, phenylalanine uptake and Michaelis-Menten kinetics of WT hLAT4 (hLAT4) and alanine (A, C) or glutamic acid (B, D) mutants of S274 and S297 or S274S278 and S278, respectively. The Michaelis-Menten curves were calculated using GraphPad Prism. Statistical analysis was performed with GraphPad Prism, using one-way ANOVA

with Bonferroni multiple comparison test. Values are means \pm 95% CI, * P < 0.05; ** P < 0.01; *** P < 0.001. Results were pooled from 3 (mutants) or 12 (WT LAT4) experiments, n = 8–10 oocytes per experiment. *E*, Western blot showing protein expression of WT hLAT4 and its phosphorylation mutants after cRNA injection in *Xenopus laevis* oocytes. All hLAT4 inserts contain a C-terminal FLAG sequence. NI: non-injected oocytes; hLAT4: WT hLAT4; S...A: alanine mutant; S...E: glutamic acid mutant. Total lysates probed with antibody against FLAG sequence. PNGaseF used as indicated (+) to deglycosylate proteins. Upper panel: representative Western blots, each lane containing pooled lysates from 8–10 oocytes. Lower panel: quantification of data pooled from 3 separate experiments. Values are means \pm 95% CI, n = 24–30.

Santa Clara, CA, USA). Primers used for mutagenesis are shown in Table 1. All constructs were linearized using PvuI enzyme. For cRNA synthesis, MEGAscript high-yield *in vitro* transcription SP6 kit was used according to manufacturer's instructions (Cat. No. AM1330, Lot No. 00306472, Ambion, Austin, TX, USA).

Handling of *Xenopus laevis* oocytes and cRNA injections

Oocyte selection from *Xenopus laevis* frogs (*Xenopus* Express Cat. No. IMP XL FM, RRID: XEP_XLFM, Xenopus Express, Vernassal, France) and buffer preparation was

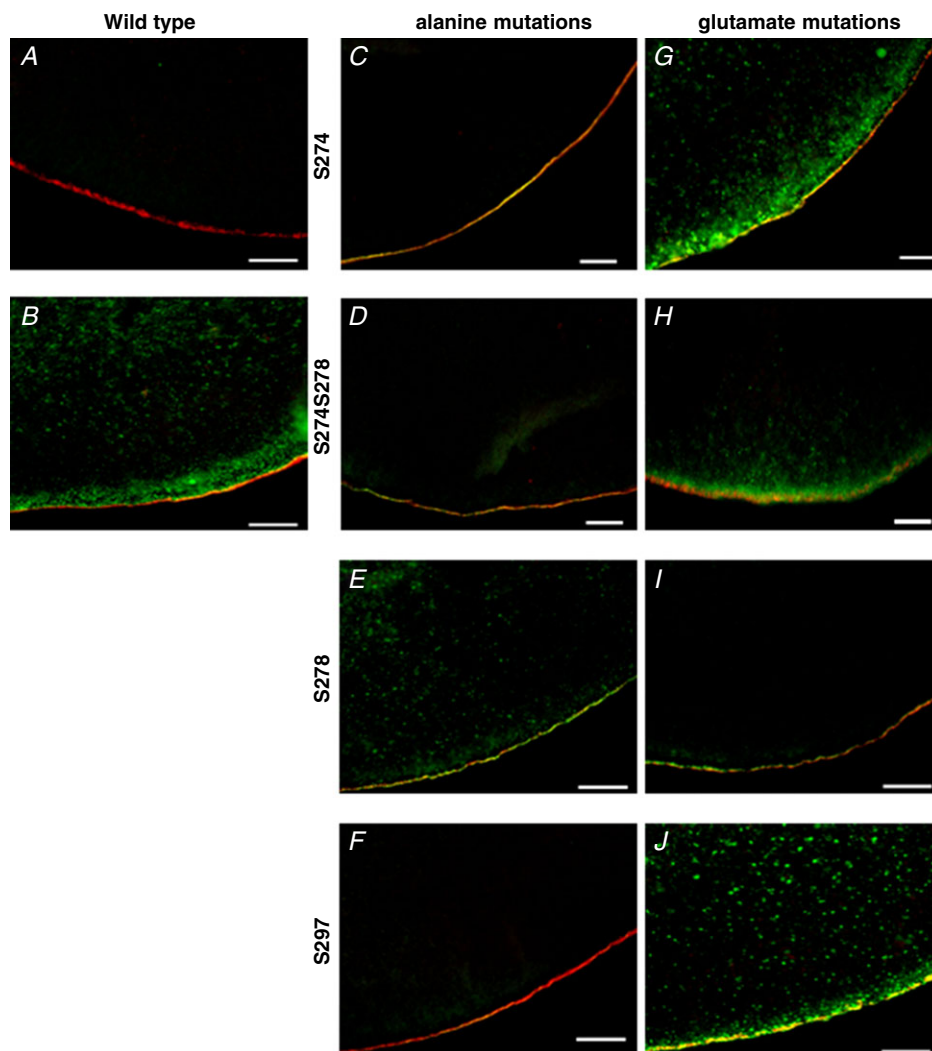


Figure 2. Dephosphorylation on S274 enhances LAT4 membrane localization visualized by immunofluorescence

A, non-injected *Xenopus laevis* oocytes. *B*, wild-type hLAT4. *C–F*, hLAT4 alanine mutants. *C*, S274A; *D*, S274AS278A; *E*, S278A; *F*, S297A. *G–J*, hLAT4 glutamic acid mutants. *G*, S274E; *H*, S274ES278E; *I*, S278E; *J*, S297E. All hLAT4 constructs contain a C-terminal FLAG sequence. Antibodies against FLAG sequence (hLAT4 detection, in green) and actin-phalloidin (membrane marker, in red) used on oocyte cryosections. Images from animal pole shown. Scale bar: 10 μ m.

done as previously described (Taslimifar *et al.* 2017). Briefly, stage IV oocytes were selected and treated with collagenase A. The remaining follicular layer was manually removed with forceps on the selection day. After 24 h, oocytes were injected with 10 ng of FLAG-tagged hLAT4 or its phosphorylation mutant cRNA. Oocytes were kept

in modified Barth's solution at 16°C for 72 h to express the constructs.

Amino acid uptake in *Xenopus laevis* oocytes

The uptake rate of L-phenylalanine (Phe) was measured in *Xenopus laevis* oocytes as described previously (Ramadan

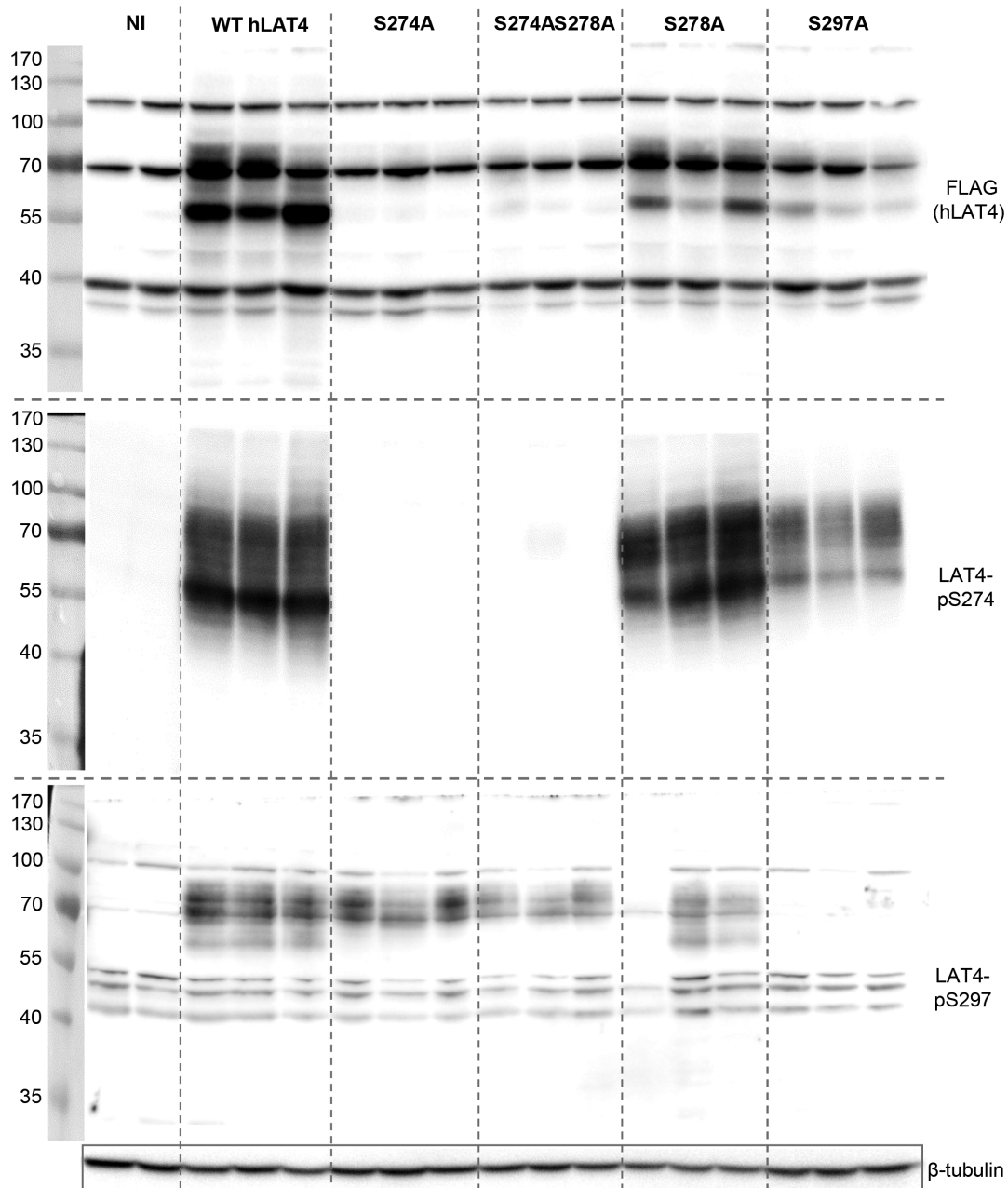


Figure 3. LAT4 is phosphorylated in *Xenopus laevis* oocyte expression system

Western blots showing protein expression and phosphorylation of WT hLAT4 and its phosphorylation mutants after cRNA injection in *Xenopus laevis* oocytes. All hLAT4 inserts contain a C-terminal FLAG sequence. Total lysates probed with antibody against FLAG sequence (upper panel), or antibody against LAT4-pS274 (middle panel) or against LAT4-pS297 (lower panel). In the middle panel, a composite image is shown from two separate blots, that contained the same WT LAT4 controls. Oocytes from two (NI = non-injected) or three (WT hLAT4 and mutants) different batches used; each lane contains pooled lysates from 8–10 oocytes.

Table 1. Primers used for mutagenesis

Site	Change	Forward	Reverse
S274	Serine (S) → alanine (A)	5'-GGC CGG CGC CTG GCT GTG GGC AGC TC-3'	5'-GAG CTG CCC ACA GCC AGG CGC CGG CC-3'
	S → glutamate (E)	5'-GTG GGC CGG CGC CTG GAA GTG GGC AGC TCC ATG-3'	5'-CAT GGA GCT GCC CAC TTC CAG GCG CCG GCC CAC-3'
S278	S → A	5'-GGC TGT GGG CAG CGC CAT GAG GAG TGC-3'	5'-GCA CTC CTC ATG GCG CTG CCC ACA GCC-3'
	S → E	5'-CCT GGA AGT GGG CAG CGA GAT GAG GAG TGC CAA GG-3'	5'-CCT TGG CAC TCC TCA TCT CGC TGC CCA CTT CCA GG-3'
S297	S → A	5'-CAA GCT GTG CCT GGC CAC CGT CGA CCT-3'	5'-AGG TCG ACG GTG GCC AGG CAC AGC TTG-3'
	S → E	5'-CCA CAA GCT GTG CCT GGA GAC CGT CGA CCT GGA GG-3'	5'-CCT CCA GGT CGA CGG TCT CCA GGC ACA GCT TGT GG-3'

et al. 2006). In each experiment, oocytes expressing either A or E mutant of the same phosphorylation site were tested in comparison with oocytes expressing wild-type (WT) hLAT4 and non-injected oocytes. Before the uptake, oocytes representing the same condition ($n = 8-10$) were pooled in a single tube and equilibrated in a water bath for 2 min at 25°C in the washing solution (100 mM NaCl, 2 mM KCl, 1 mM CaCl₂, 1 mM MgCl₂, 10 mM HEPES-Tris, pH 7.4). Afterwards, the washing solution was aspirated and 100 μ l of uptake solution was added. The uptake solution consisted of washing buffer, 5 μ Ci/ml of [³H]-L-radiolabelled (tracer) Phe (Cat. No. MT1916, Hartmann Analytic GmbH, Braunschweig, Germany), and non-labelled Phe at one of the following concentrations: 0.0033, 0.010, 0.033, 0.10, 0.33, 1.0, 3.3 or 10 mM. Oocytes were incubated in the uptake solution for 10 min at 25°C. Then the uptake solution was aspirated and oocytes were washed five times with 2 ml of ice-cold washing buffer. After washing, oocytes were distributed into separate tubes and dissolved with 250 μ l of 2% SDS using agitation for at least 1 h. Once dissolved, 3 ml of scintillation fluid Emulsifier-Safe was added (Cat. No. 6013389, Lot No. 76-17041, Perkin Elmer, Schwerzenbach, Switzerland) and radioactivity determined in a TRI-CARB 2900TR (Packard Instruments, Meriden, CT, USA) liquid scintillation counter. Uptake values were corrected by subtracting radioactivity levels from the remaining washing solution, accounting for the counter background and tracer potentially carried over with the washing solution. Finally, the counts measured in non-injected (NI) oocytes submitted to the same uptake procedure were also subtracted. This latter background represents the uptake of phenylalanine by endogenous *Xenopus* oocyte transporters which is quite elevated and strongly concentration dependent. We have previously shown that this endogenous uptake is mediated by various transporters with different K_m , specifically xB⁰AT1 (SLC6A19), xATB^{0,+} (SLC19A14), xLAT4 and xTAT1 (Taslimifar *et al.* 2017). The uptake experiment for each mutant pair including WT LAT4 and NI controls was repeated three times using different batches of oocytes.

Fixation of *Xenopus laevis* oocytes for immunofluorescence

Oocytes either expressing hLAT4 or its mutants, or in their native state were transferred to a 6-well plate 72 h after cRNA injections and washed three times with 2 ml of ice-cold phosphate buffered solution (PBS). After this the oocytes were incubated in 2 ml of 3% paraformaldehyde (PFA) in PBS for 4 h at 4°C. Then the PFA-PBS solution was replaced by a 30% sucrose-PBS solution, in which the oocytes were incubated overnight at 4°C. The sucrose solution was then aspirated and the oocytes were incubated in PBS for 15 min at 25°C. Subsequently they were embedded in OCT Embedding Matrix (Cat. No. 81-0771-00, Lot No. 03810561, CellPath Biosystems, Muttens, Switzerland), snap frozen using liquid propane and stored at -80°C.

Fixation of small intestine for immunofluorescence

Harvested small intestines (duodenum and jejunum) were cut open and flattened, then fixed for 1 h in 4% PFA-PBS at 4°C. The intestines were then 'Swiss-rolled' (Moolenbeek & Ruitenbergh, 1981) and fixed overnight in 4% PFA-PBS at 4°C. After fixation, the rolls were washed with PBS for 3 h, then incubated with 15% sucrose for 5 h, followed by an overnight incubation in 30% sucrose, all at 4°C. After this the intestinal rolls were placed into a 30% sucrose-OCT mix (1:1 ratio) for 1 h at room temperature before embedding on dry ice. Fixation of ileum was done in the same way, however, it was not 'Swiss-rolled', but cut into several rings instead.

Immunofluorescence

For colocalization of hLAT4 and actin phalloidin, 7 μ m sections were prepared from OCT embedded oocytes. Consecutive 3 μ m sections were prepared from duodenal and jejunal Swiss rolls and ileal rings. In both cases Superfrost[®] Plus Menzel slides (Cat. No. J1800AMNJ, Lot No. 041217, Gerhard Menzel GmbH, Braunschweig, Germany) were used. Sections were rehydrated in PBS

for 15 min at room temperature. Intestinal sections used for on-slide dephosphorylation were then incubated with either Lambda protein phosphatase (Lambda PP) (Cat. No. P0753, Lot No. 0071610, New England Biolabs, Ipswich, MA, USA) or phosphatase inhibitor cocktail (Cat. No. 100567, Lot No. 11117006, Active Motif, La Hulpe, Belgium) in buffers provided with the Lambda PP kit for 30 min at 30°C. After rehydration or dephosphorylation, sections were washed for 5 min: twice with PBS and once with hypertonic PBS (+18 g/l NaCl). No epitope retrieval was performed. After washing, sections were incubated in the blocking solution (2% bovine serum albumin, 0.04% Triton X-100 in PBS, pH 7.4) for 1 h at room temperature. Primary antibodies were also diluted in the blocking solution and incubated overnight at 4°C. Dilutions used were: anti-FLAG 1:1000, anti-LAT4 1:1500, anti-pS274 1:1000, anti-E-Cadherin 1:300. Then sections were washed as before and incubated with secondary antibodies diluted 1:2000 in blocking solution for 1 h at room temperature. Together with the secondary antibodies, nuclei staining (DAPI, 1:5000) and membrane staining for oocytes (X-phalloidin, 1:500) was performed. Afterwards, sections were washed again and fixed using Glycergel mounting medium (Cat. No. C0563, Lot No. 1012846, Agilent Technologies, Santa Clara, CA, USA). All samples were imaged using fluorescent light microscopes (Zeiss Axiovert 200 for oocytes, Nikon Eclipse TE 300 and Leica SP5 confocal for intestinal sections).

Image analysis

Nuance 3.0.2. FX Multispectral Imaging system was used (Nuance Multispectral Imaging Systems, RRID:SCR_015382, Perkin Elmer, Schwerzenbach, Switzerland) to eliminate the strong oocyte auto-fluorescence in acquired images. Fluorescence spectra from non-stained oocyte sections were sampled and then unmixed and removed from the spectra of the stained sections according to the manufacturer's instructions.

To assess phosphorylation differences along the intestinal villus, its length was measured in the acquired IF images and then split into three identical parts: tip, middle and base. The average fluorescence intensity of each part was measured for the different colour channels. Values given by LAT4 or phosphorylation site-specific antibodies were then related to the fluorescence intensity of the membrane marker E-Cadherin. Exposure time, gain, brightness and contrast were kept constant for all tissue sections stained with the same antibody. Only full length villi that were not damaged or segmented by section cutting and processing were used for measurements and analysis; $n = 5-7$ villi per intestinal segment per mouse. All measurements were done using ImageJ 1x software (National Center for Microscopy and Imaging Research:

ImageJ Mosaic Plug-ins, RRID:SCR_001935) (Schneider *et al.* 2012).

Western blotting

Oocytes expressing the same construct were pooled ($n = 8-10$) and lysed in cold lysis solution (250 mM sucrose, 0.5 mM EDTA, 5 mM Tris HCl pH 6.9; 10 μ l per oocyte) supplemented with protease inhibitor cocktail (Cat. No. P8340, Lot No. 126M4016V, Sigma-Aldrich). Homogenization was done by passing oocytes through a 25G needle. Afterwards the total lysate was centrifuged at 100 g for 10 min at 4°C, the supernatant (below the fat ring) transferred to another tube and the centrifugation step repeated to yield fat-free total lysate.

To prepare the total intestinal membranes, still-frozen scraped jejunal mucosa was homogenized for 20 s at 5500 rpm (Precellys24, Bertin Instruments, Montigny-le-Bretonneux, France) in 400 μ l mannitol resuspension buffer (200 mM D-mannitol, 80 mM HEPES, 41 mM KOH, pH 7.5) with supplemented protease inhibitor and phosphatase inhibitor cocktails. The homogenate was centrifuged at 2000 g for 15 min at 4°C to sediment cellular debris. The supernatant was then ultracentrifuged at 41,000 rpm for 1 h at 4°C (rotor RP45A, Sorvall, ThermoFisher Scientific, Waltham, MA, USA) and the pellet resuspended in 50 μ l mannitol resuspension buffer using a tip sonicator (Labsonic 1510, Bender&Hobein, Zurich, Switzerland). Samples were processed in groups of twelve with random assortment.

To determine the effects of sample preparation on proteolytic fragmentation of mLAT4, small intestine after harvesting was immediately washed with ice-cold PBS containing protease and phosphatase inhibitor cocktails. After this the jejunum was separated and cut into three equal parts that were cut open longitudinally. From two parts the mucosa was removed by scraping with a surgical scalpel or glass coverslip. The third part was incubated for 30 min at 37°C in EDTA solution (5 mM EDTA, 1 \times HBSS, 1 mM DTT, protease and phosphatase inhibitor cocktails), then passed through a 100 μ M cell strainer to collect the mucosal cells. Preparation of total lysates was done either by homogenization (Precellys24, Bertin Instruments), or by passing through a 25G needle. Either mannitol or modified RIPA (150 mM NaCl, 50 mM Tris-HCl pH7.4, 1 mM EDTA, 1% Triton-X100, 1% sodium deoxycholic acid) lysis buffers containing protease and phosphatase inhibitor cocktails were used. The homogenate was then processed for total membrane preparation as described above.

The protein concentration in the samples was determined using DC-Protein Assay (Cat. No. 23228, Lot No. SG249029, ThermoFischer Scientific, Rockford, IL, USA) according to the manufacturer's instructions. Afterwards protein samples in chosen concentrations

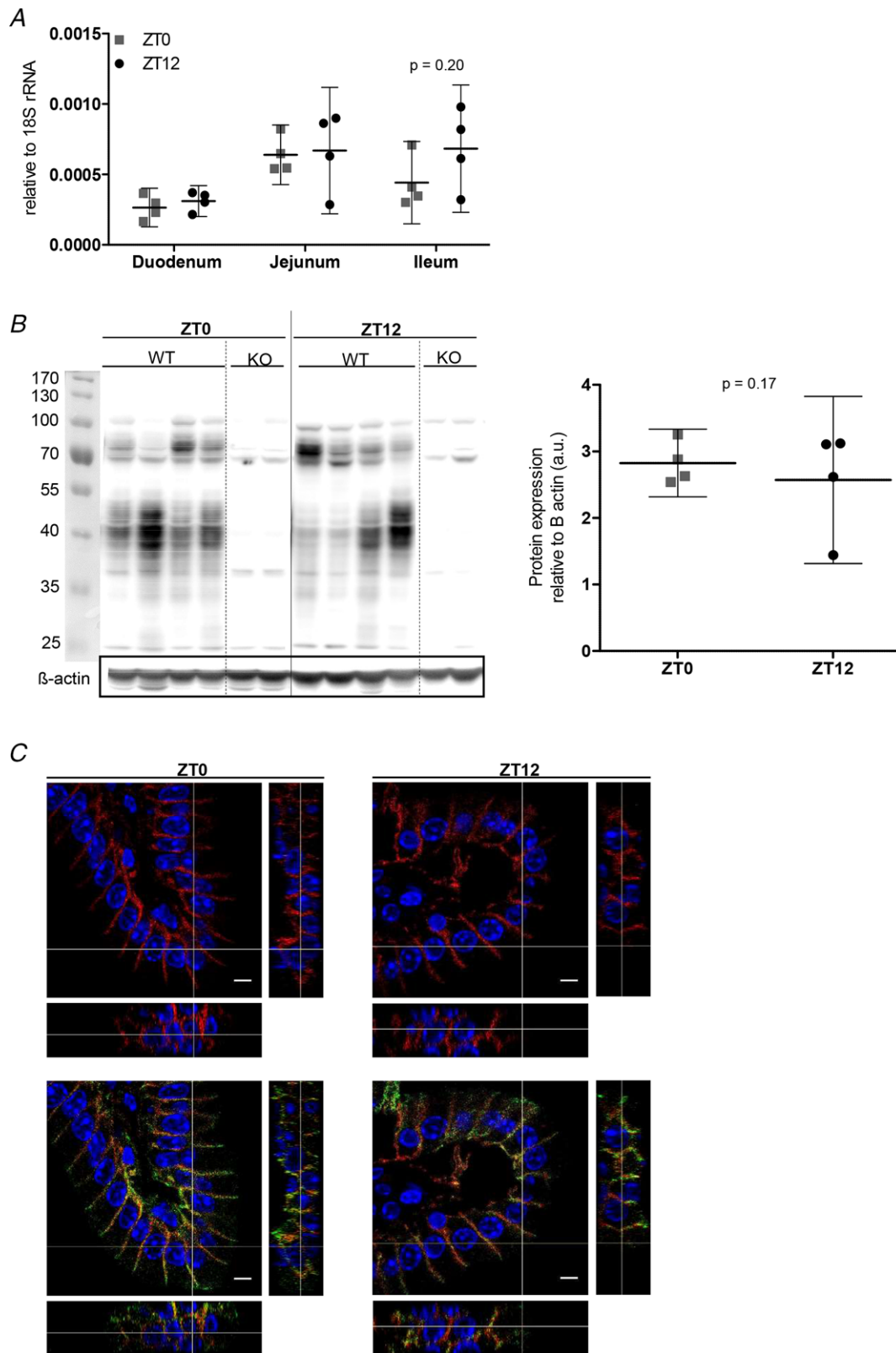


Figure 4. LAT4 mRNA and protein expression and localization *in vivo* is not dependent on food entrained diurnal rhythm

Wild-type mice were put on time-restricted feeding regime. ZT0: start of the passive period, 4 h after food removal. ZT12: start of the active period, end of 16 h starvation period. A, mRNA expression of LAT4 along the small intestine

measured by real time RT-PCR. Values are means \pm 95% CI, $n = 4$. B, LAT4 protein expression in jejunum. Total membrane lysates from jejunum of wild-type (WT) and conditional LAT4 knockout (KO) mice analysed by Western blot using anti-LAT4 antibody. LAT4 appears as a band migrating above 70 kDa and proteolytic fragments between 55 and 30 kDa (see Fig. 5). Quantification of its expression relative to the β -actin expression level is shown in the right panel. Statistical analysis performed with Student's unpaired t test. Values are means \pm 95% CI, $n = 4$. C, LAT4 localization in jejunal villi visualized by immunofluorescence. Upper panel: LAT4 (in red), lower panel: membrane marker E-cadherin (in green) and LAT4 (in red). Scale bar: 8 μ m.

were diluted in 4 \times Laemmli buffer containing 10% β -mercaptoethanol. Samples were then incubated at room temperature for 20 min and loaded on 1 mm 10% polyacrylamide gels. Separation was done by electrophoresis and a PVDF membrane (Cat. No. IPVH00010, Immobilon-P, Merck Millipore, Burlington, MA, USA) was then used for wet transfer. Membranes were blocked for 1 h at room temperature with either 5% milk powder in Tris-buffered saline containing 0.1% Tween-20 (TBS-Tween) or with 2% TopBlock (Cat. No. TB232010, Lot No. 206008, LuBioscience, Lucerne, Switzerland) in TBS-Tween. Primary antibodies were diluted in 5% milk powder-TBS-Tween (anti-LAT4 1:2000 and anti-FLAG 1:1000) or 2% TopBlock-TBS-Tween (anti-pS274 1:500, anti-pS297 1:300) and incubated overnight at 4°C. Afterwards blots were washed in TBS-Tween for 3 \times 5 min and secondary antibodies applied in the same solutions at a 1:5000 dilution and incubated for 1 h at room temperature. β -Actin (intestinal mucosa) or β -tubulin (oocytes) were

used as loading controls, both antibodies being applied at a 1:5000 dilution. Antibody binding was detected using Luminata Classico Western Chemiluminescent HRP substrate (Cat. No. WBLUC0100, Lot No. 163273, Merck Millipore, Burlington, MA, USA) or CDP-Star substrate (Cat. No. NIF1229, Lot No. 13861046, GE-Healthcare UK, Bucks, UK). Blots were imaged with ImageQuant (ImageQuant, RRID:SCR_014246) LAS 4000 camera (Fujifilm, Tokyo, Japan). Densitometric analysis was performed on original blots with ImageJ 1x software. For visualization purposes the brightness and contrast of the whole image in Figs 1E, 3, 4B, 5, 6C–E and 7A was adjusted using ImageJ.

RNA extraction and real-time PCR

Freshly harvested mouse intestine was placed on an ice-cold surface, and 1–2 cm from duodenum, jejunum and ileum was cut off, everted and scraped with a

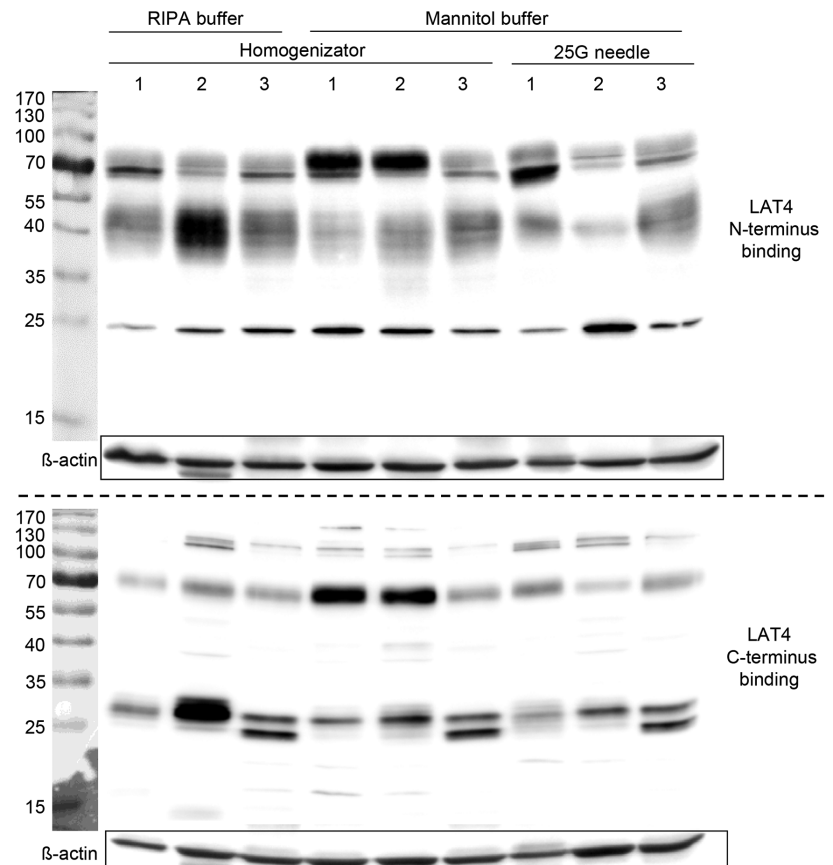


Figure 5. Proteolytic fragmentation of LAT4 visualized on Western blot using antibodies binding to its NH₂- (upper panel) or COOH-terminus (lower panel)

Intestinal mucosa of WT mice jejunum was collected by scraping with surgical scalpel (1), by scraping with glass coverslip (2) or collected after mucosa cell detachment in EDTA buffer (3).

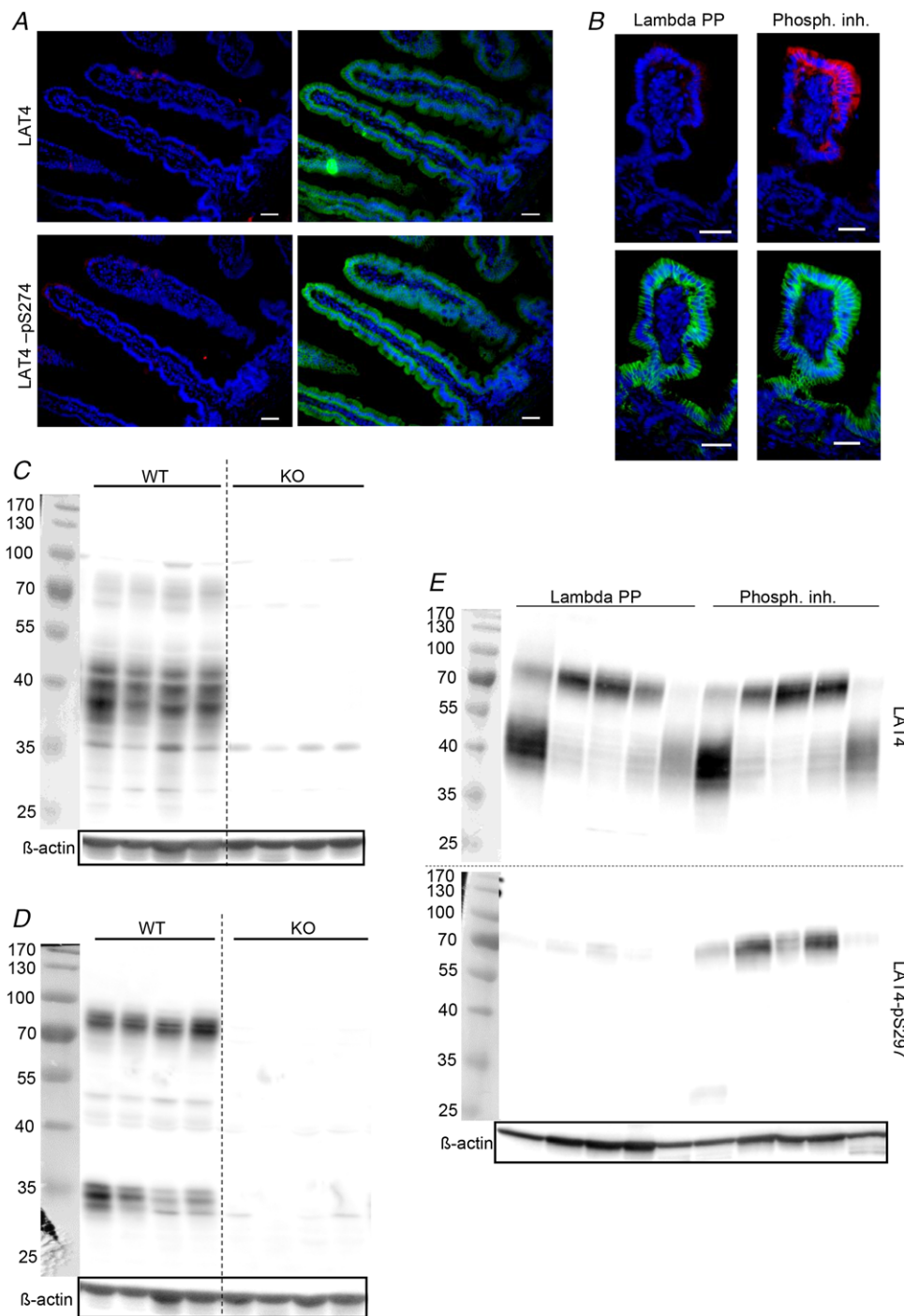


Figure 6. LAT4 and phosphosite antibody specificity

A, near absence of enterocytes labelled with anti-LAT4 (upper panel, in red) and anti-pS274 (lower panel, in red) antibodies on jejunum cryosections of LAT4 conditional knockout mice confirms LAT4 specificity of both antibodies and efficiency of LAT4 knockout. Green: E-Cadherin; blue: DAPI. Scale bar: 30 μm . **B**, near absence of labelling with anti-pS274 antibody (in red) on jejunal cryosection incubated with Lambda protein phosphatase (left panel), in contrast to the section incubated with phosphatase inhibitor cocktail (right panel), confirms phospho-specificity of antibody. Green: E-Cadherin; blue: DAPI. Scale bar: 30 μm . **C** and **D**, specificity of LAT4 (**C**) and pS297 (**D**) antibody. Membrane protein lysates from duodenum of wild-type (WT) and LAT4 conditional knockout (KO) mice were analysed by Western blot. **E**, phospho-specificity of pS297 antibody. Membrane protein lysates from jejunum of wild-type (WT) mice treated with Lambda protein phosphatase (Lambda PP) or phosphatase inhibitor cocktail (Phosph. inh.) were analysed by Western blot. Signal obtained with pS297 antibody is strongly decreased after phosphatase treatment, unlike that with LAT4 antibody.

surgical scalpel to isolate the mucosa. The scraped mucosa was immediately frozen in liquid nitrogen. Total RNA was extracted using RNeasy Mini Kit (Cat. No. 74106, Lot No. 157057561, Qiagen, Hombrechtikon, Switzerland) according to the manufacturer's instructions. The quality and quantity of the extracted RNA were

assessed using an RNA 600 Nano kit (Cat. No. 5067-1511, Lot No. KF04BK03, Agilent Technologies, Santa Clara, CA, USA) and spectrophotometry, respectively. Reverse transcription was performed with a qScript cDNA synthesis kit (Cat. No. 95047, Lot No. 020927, Quantabio Inc., Beverly, MA, USA) using 500 ng of RNA as template.

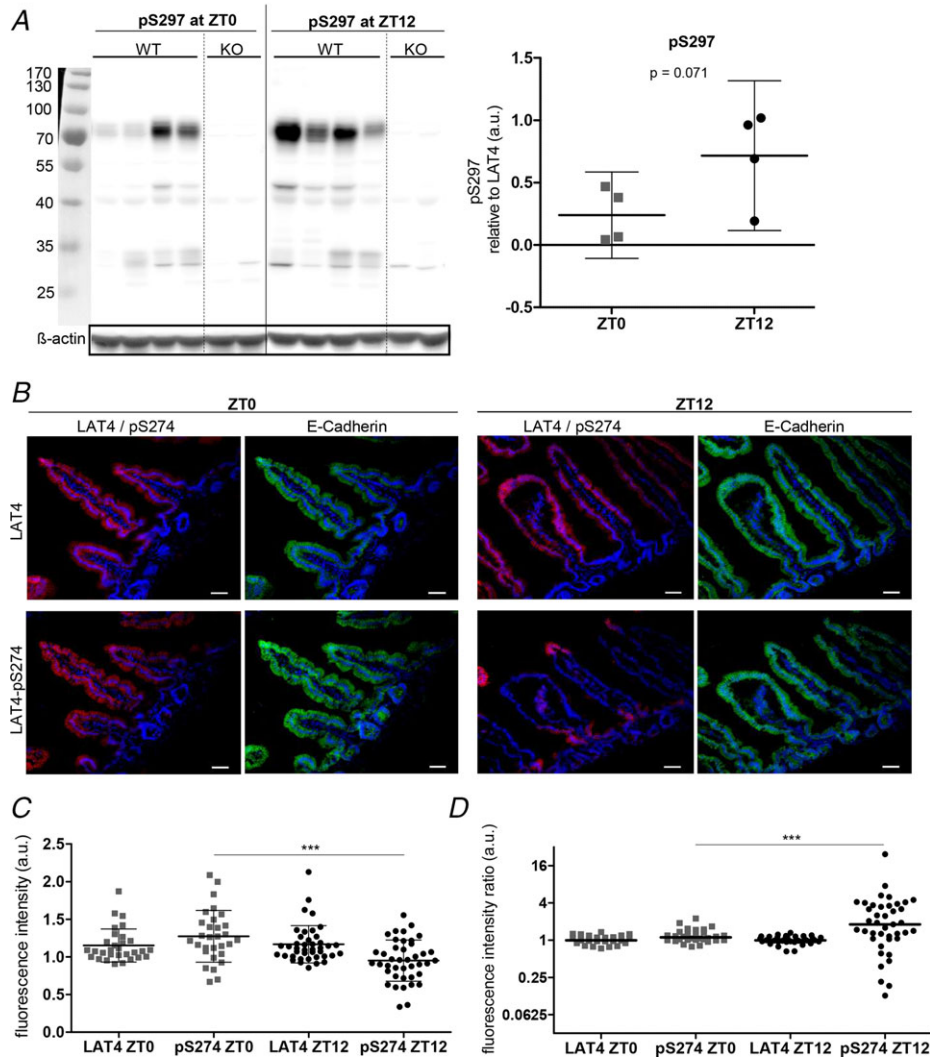


Figure 7. LAT4 phosphorylation changes suggest an increase in its function with food anticipation
 Wild-type mice were put on time-restricted feeding regime. ZT0: start of the passive period, 4 h after food removal. ZT12: start of the active period, end of 16 h starvation period. **A**, LAT4 phosphorylation on S297. Total membrane lysates from jejunum of wild-type (WT) and conditional LAT4 knockout (KO) mice analysed by Western blot. Phosphorylation relative to the total LAT4 expression level. Statistical analysis performed with Student's unpaired *t* test. Values are means \pm 95% CI, *n* = 4. **B**, LAT4 expression and phosphorylation on S274 in mice jejunum. Red: LAT4 or pS274; green: E-Cadherin; blue: DAPI. Scale bar: 30 μ m. **C**, average fluorescence intensity in jejunal villi. Values are means \pm SD, *n* = 20–30 villi. **D**, fluorescence ratio between the tip and middle part of jejunal villi. Logarithmic scale used. 1: same fluorescence intensity on tip and middle part; > 1: fluorescence intensity is increased on tip; < 1: intensity lower on tip. Values are medians, *n* = 20–30 villi. For **C** and **D** villi were stained with antibodies against LAT4 or pS274, and membrane marker E-cadherin. Fluorescence intensity determined with ImageJ 1x software and related to intensity of E-cadherin. Statistical analysis: one-way ANOVA with Bonferroni multiple comparison test, ****P* < 0.001. **E**, LAT4 expression and phosphorylation on S274 in duodenum at the start of the active phase (ZT12). Red: LAT4 or pS274; green: E-Cadherin; blue: DAPI. Scale bar: 40 μ m. **F**, schematic representation of distribution of S274 phosphorylation on mouse jejunal and duodenal villi. **G**, strong decrease of pS274 labelling on small ileal villi at the start of active period. Red: LAT4 or pS274; green: E-Cadherin; blue: DAPI. Scale bar: 15 μ m.

For real-time (RT) PCR 75 ng cDNA, TaqMan Universal PCR Mastermix (Cat. No. 4304437, Lot No. 1801137, Applied Biosystems, Waltham, MA, USA) and other reaction components were mixed in accordance with the manufacturer's instructions. Primers and probes for LAT4 were as described previously (Guete *et al.* 2015). The probe was labelled with the reporter dye FAM at the 5' end and the quencher dye TAMRA at the 3' end (Microsynth, Balgach, Switzerland). The abundance of the target mRNAs (test RNA) was normalized relative to the 18S ribosomal RNA (18S RNA). All reactions were performed in triplicate and relative expression ratios were calculated as $R = 2^{-(Ct(\text{test RNA}) - Ct(18S \text{ RNA}))}$, where Ct is the cycle number at the threshold for the tested mRNAs.

Statistics

Experimental data analysis was performed using GraphPad Prism v5.0 (Graphpad Prism, RRID:SCR_002798, Graphpad software, San Diego, CA, USA). Michaelis-Menten curve fitting and calculation of kinetic parameters was done using the Michaelis-Menten non-linear fit equation with least squares (ordinary) fit. Differences between the mean values of groups were assessed with a Student's unpaired *t* test or one-way

analysis of variance (ANOVA) followed by a Bonferroni multiple comparison test, as indicated in the figure legends. Regarding *Xenopus laevis* oocytes, all statistical tests were done using NI and WT LAT4 controls from the respective experimental triplicates (both controls and one mutant pair tested in the same experiment, repeated 3 times, $n = 25\text{--}30$ oocytes); however, for visualization purposes in Fig. 1A–1D and Table 2, WT LAT4 results are pooled from all experimental triplicates ($n = 110\text{--}120$ oocytes). Levels of significance were shown as: * $P < 0.05$; ** $P < 0.01$; *** $P < 0.001$. Data are shown as mean values with standard deviations (SD), mean values with 95% confidence intervals (95% CI) or median values, as indicated in the figure legends.

Results

Testing the impact of (non-)phosphorylation mimicking mutants on LAT4 kinetics in *Xenopus laevis* oocytes

To assess whether the phosphorylation state may affect hLAT4 expression and/or function, we mutagenized the phosphorylation sites S274, S278 and S297 separately, as well as S274 and S278 together (S274S278), to

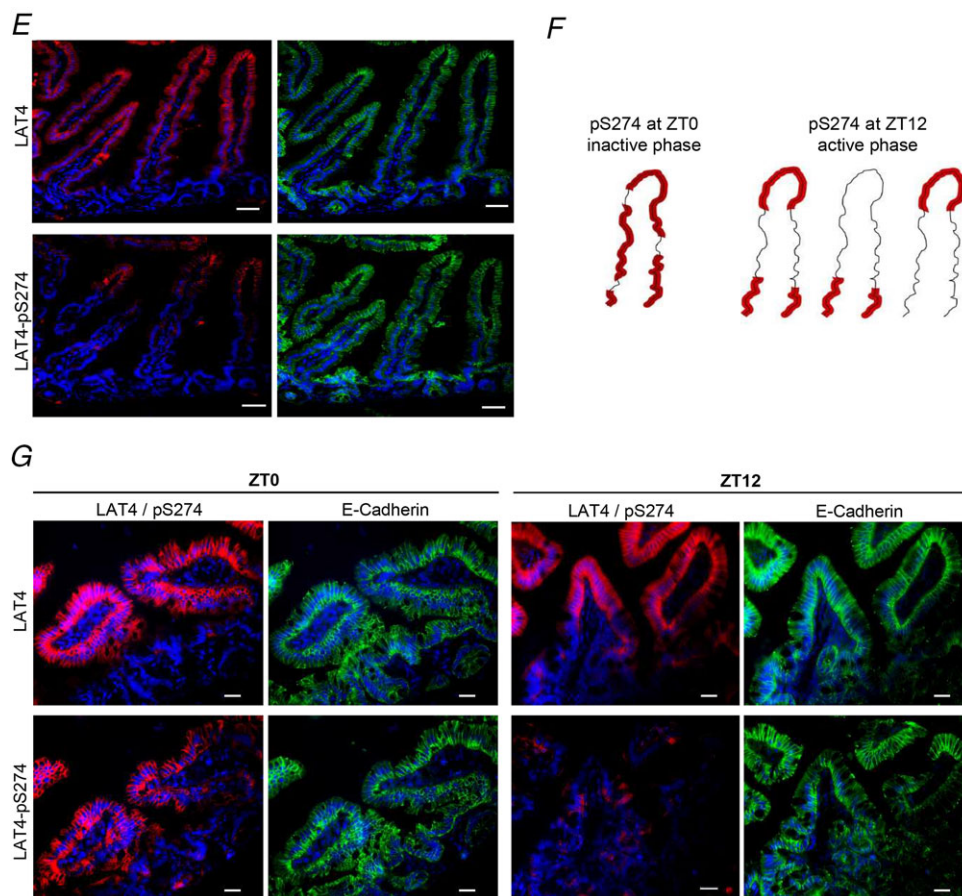


Figure 7. Continued

Table 2. Phenylalanine transport kinetics by LAT4 and its phosphorylation site mutants expressed in *Xenopus laevis* oocytes

	WT LAT4	S274A	S278A	S274A S278A	S274E	S278E	S274E S278E	S297A	S297E
Phe uptake rate ^a (pmol/10 min)	72.6 ± 22.6	112.7 ± 29.2	45.4 ± 11.7	77.2 ± 29.1	45.6 ± 16.2	54.7 ± 12.8	60.8 ± 12.2	17.7 ± 12.1	41.4 ± 23.2
K_m^b (mmol/l)	6.2 ± 0.8	2.4 ± 0.4	2.3 ± 0.5	4.1 ± 0.6	7.5 ± 1.6	4.4 ± 0.8	2.4 ± 0.3	7.2 ± 3.6	13.4 ± 5.7
V_{max} (pmol/10 min)	444.8 ± 27.1	358.0 ± 23.8	195.5 ± 14.3	390.4 ± 22.9	314.9 ± 34.2	307.7 ± 23.6	197.6 ± 8.99	77.8 ± 19.7	416.8 ± 31.0

^aPhenylalanine (Phe) was given at a concentration of 1 mmol/l. Results pooled from 3 (mutants) or 12 (WT LAT4) separate experiments. Values are means ± SD, n = 8–10 oocytes per experiment.

^bMichaelis-Menten curve fitting and corresponding apparent affinities (K_m) and maximal transport velocities (V_{max}) were calculated using GraphPad Prism.

either alanine (A) or glutamate (E), in order to mimic the non-phosphorylated (also dephosphorylated) or phosphorylated states, respectively. We then expressed these constructs in *Xenopus laevis* oocytes and first tested their function using phenylalanine (Phe) as uptake substrate. It has to be mentioned that the transporter function measured as uptake rate depends on both transporter expression level and functional state at the cell surface.

All phosphorylation-mimicking glutamate mutants of hLAT4 displayed a trend towards slightly lower uptake rates (pmol/10 min) and/or maximal transport velocities (V_{max} , pmol/10 min) of Phe at 1 mM, compared to wild-type (WT) hLAT4 (Fig. 1B and D, Table 2).

In contrast to glutamate mutants, most alanine mutants showed strong site-specific effects (Fig. 1A and C, Table 2). For instance, the uptake rate of Phe at several tested concentrations and the apparent affinity of Phe (reciprocal value of K_m for Phe transport rate, in mmol/l) were clearly increased by the S274A mutation (Fig. 1A, Table 2). The alanine mutation of S278 similarly increased the apparent affinity of LAT4 for Phe, but it also substantially decreased V_{max} . Thus the uptake rate at relevant Phe concentrations was actually slightly decreased, reaching a similar level to that observed with the S278E mutant (Fig. 1C and D, Table 2). The transport function of the double mutant S274AS278A was nearly identical to that of WT hLAT4 (Fig. 1C, Table 2).

These results suggest that LAT4 is more active at the cell surface when position S274 is dephosphorylated. As regards position S278, the functional impact of its phosphorylation state is less clear, but we can speculate that it affects the (de)phosphorylation of S274.

In contrast, the dephosphorylation-mimicking alanine mutation in position S297 led to a severe reduction of Phe uptake rate by hLAT4, essentially by decreasing its V_{max} and thereby strongly reducing its transport rate at relevant substrate concentrations (Fig. 1A, Table 2). Interestingly, the phosphorylation-mimicking glutamate mutation S297E caused a decrease in Phe apparent affinity, but maintained V_{max} , also leading to a lower Phe uptake rate (Fig. 1B, Table 2). Thus, these findings suggest that phosphorylation or dephosphorylation of hLAT4 at the positions S274 and S297 play important, mostly opposite roles in regulation of the transport function. Indeed, an increased LAT4 function was observed when dephosphorylation of S274 was mimicked, whilst mimicking dephosphorylation of S297 led to a major decrease in LAT4 function.

Testing the impact of (non-)phosphorylation mimicking mutants on hLAT4 protein expression and localization in *Xenopus laevis* oocytes

To test whether phosphorylation affects hLAT4 protein expression levels, we performed Western blotting (WB)

using total lysate of native *Xenopus* oocytes (NI, non-injected) and of oocytes expressing FLAG-tagged wild-type or mutant hLAT4. Exogenous hLAT4 appeared as multiple fuzzy bands migrating between 80 and 58 kDa (Fig. 1E). Upon deglycosylation with PNGaseF, hLAT4 migrated as a major and strongly labelled band at approximately 55 kDa, confirming that hLAT4 is glycosylated in this expression system (as shown previously in Bodoy *et al.* 2005) and suggesting that the bands migrating between 80 and 58 kDa represent terminally and core-glycosylated forms of the transporter, respectively. Compared with WT hLAT4, all alanine mutants, except S278A, displayed weaker band intensities suggesting a destabilization of the transporter. In contrast, glutamate mutants, with the exception of the double-mutant S274ES278E, preserved stronger band intensities, in particular when de-glycosylated. Some of the mutants were hardly detectable on Western blots unless their signal was more focused after deglycosylation (S274A, S297A and S274ES278E). For mutant S274AS278A, the band detected with the anti-FLAG antibody was so weak even after deglycosylation that it is not visible in Fig. 1C. However, its fully glycosylated form was clearly detected with an anti-LAT4-pS297 antibody (see below and Fig. 3). Together, these results suggest that phosphorylation in positions S274 and S297 tend to stabilize hLAT4 in *Xenopus* oocytes, in the case of S297 stabilizing specifically the terminally glycosylated mature form.

Using immunofluorescence, we visualized the localization of hLAT4 and its mutants in *Xenopus* oocytes also labelled with phalloidin to stain the actin filaments present in the membrane infoldings. In non-injected oocytes only this submembranous labelling with phalloidin was visible (Fig. 2A, in red). Exogenous WT hLAT4 (in green) localized mostly in an intracellular (IC) pool close to the membrane, with only a small fraction present at the membrane, as shown by the co-localization (in yellow) with the actin marker phalloidin (Fig. 2B). Interestingly, the S274A and S274AS278A mutants were nearly absent from the IC pool and their overall expression was strongly reduced (Fig. 2C and D), as seen also in Western blots in which their core-glycosylated form was hardly visible (Fig. 1E). However, these alanine mutants displayed an increased membrane localization (co-localization with phalloidin in orange/yellow, Fig. 2C and D). In contrast, the alanine mutation of the nearby S278 had only a relatively small effect on the total amount and the localization of the transporter compared to the wild type (Figs 1E and 2E).

The alanine mutation of S297 had a strong effect, reducing the expression level of hLAT4 in the IC pool similarly to S274A, and, in addition, reducing its surface expression (Figs 1E and 2F). Unlike the alanine mutations, glutamate mutations in general did not affect the localization of hLAT4 compared to the wild-type

transporter (Fig. 2G–J), with the exception of S278E (Fig. 2I).

The fact that the non-phosphorylation mimicking alanine mutation of S274 strongly affected the localization of LAT4 and the alanine mutation of S297 affected both its localization and its function suggests that wild-type LAT4 may be to a large extent phosphorylated on both of these sites in *Xenopus* oocytes. Results obtained by Western blotting performed with phosphorylation site-specific antibodies against phosphorylated S274 (pS274) and phosphorylated S297 (pS297) supported this hypothesis (Fig. 3). The specificity of these antibodies had first been demonstrated on total membranes from jejunum of LAT4 conditional knockout mice (Fig. 6). Indeed, WT hLAT4 expressed in *Xenopus laevis* oocytes showed phosphorylation on both serines, with stronger pS274 labelling in the lower, core-glycosylated band and, in contrast, stronger pS297 labelling in upper, terminally glycosylated bands. Interestingly, S278A and S297A mutants showed strong pS274 labelling in the upper bands, despite hLAT4 S297A mutant expression being barely detectable with anti-FLAG antibody, suggesting that the relatively low amount of hLAT4 expressed in these conditions was mainly terminally glycosylated and that the FLAG antibody had a lower binding efficiency compared to the phosphorylation site-specific ones. In S274A and S274AS278A mutants, a lower amount of the terminally glycosylated hLAT4 and a lack of core-glycosylated hLAT4 was observed with pS297 labelling, compared to the WT and S278A mutant (Fig. 3). However, one of the S278A mutants did not show any phosphorylation on S297 at all. We also have to mention that due to the strong ~70 kDa non-specific band observed with FLAG staining, proper quantification of these data was impossible.

Nevertheless, taken together these results show that mimicking dephosphorylation of S274 or S297 leads to a decrease in the immature, core-glycosylated hLAT4 and thereby to a proportional increase in its mature, terminally glycosylated form. Importantly, this mature hLAT4 appeared to be reciprocally phosphorylated on its non-mutated site (S297 or S274, respectively). In contrast, the S278 dephosphorylation mimicking mutation only slightly decreased total LAT4 expression levels but nonetheless supported the phosphorylation of its terminally glycosylated form on both S274 and S297.

Diurnal rhythm and food entrainment do not regulate the expression level and localization of jejunal LAT4 in mice

To investigate whether mRNA and protein expression and localization of LAT4 depend on diurnal rhythm, we entrained mice to scheduled feeding (time restricted feeding, TRF) with an 18% protein diet given for 8 h during the dark phase only (ZT12 to ZT20). Intestinal

samples were collected at the start of the passive period (light phase, ZT0), which was 4 h after food removal, and at the start of the active period (dark phase), when food intake is expected (ZT12).

As shown in Fig. 4A, no significant difference in mouse LAT4 (mLAT4) mRNA expression in different segments of small intestine of TRF-mice was observed between ZT0 (post-absorptive phase) and ZT12 (food expectation). On Western blots, mLAT4 appeared as multiple bands distributed between ~80 and 30 kDa; specificity of the signal was confirmed using conditional LAT4 knockout mice (Figs 4B and 6C). The presence of the lower molecular mass bands (~55–30 kDa) was not dependent on sample collection process, homogenization method or lysis buffer, indicating that these bands correspond to proteolysis products of mLAT4 (as visualized by antibodies recognizing either the N or C terminus, Fig. 5), which are most likely to be generated in the intact intestinal tissue prior to sample extraction. Thus, to measure mLAT4 expression, we quantified the intensity of all specific bands. These measurements revealed no difference in mLAT4 protein expression between ZT0 and ZT12 in jejunum (Fig. 4B). Notably, at ZT12 mice showed higher individual variances in mLAT4 protein expression. We observed the same trend for duodenum and ileum (data not shown). At both time points LAT4 appeared to similarly localize to the basolateral membrane of enterocytes of jejunal villi (Fig. 4C, in red), as shown by co-localization (in orange/yellow) with the basolateral membrane marker E-Cadherin (Fig. 4C, in green). The similarity between these two time points suggests that expression and localization of intestinal mLAT4 protein does not vary with diurnal rhythm and food entrainment.

Changes in S274 and S297 phosphorylation levels suggest an increase in jejunal mLAT4 function during food anticipation

We used phosphorylation site-specific antibodies to measure phosphorylation levels of mLAT4 in jejunum and ileum of food-entrained mice. The LAT4 specificity of pS274 (IF) and pS297 (WB) antibodies was tested in the small intestine of mice as shown in Fig. 6A, C and D. Also, in the *Xenopus laevis* oocyte expression system, mutation to alanine of the respective phosphorylation sites on hLAT4 or using native oocytes expressing no hLAT4 led to the absence of antibody binding, indicating recognition of hLAT4 and the correct epitope (Fig. 3). To test the phospho-specificity of these antibodies, dephosphorylation with Lambda protein phosphatase was used on mouse jejunal cryosections and total membrane lysates. This treatment strongly decreased the signal from phosphorylation site-specific antibodies indicating considerable phosphospecificity (Fig. 6B and E).

At the start of the active phase we observed a trend towards a pS297 WB signal increase in jejunum (Fig. 7A), and similar trends were observed in duodenum and ileum, but with even higher individual variances in duodenum (data not shown). In contrast, phosphorylation on S274 visualized by IF was clearly lower at ZT12 and limited to patches of cells mostly localized to the villus tip and/or base, observed in both jejunum and duodenum (Fig. 7B–F). An even stronger decrease in pS274 levels was observed at ZT12 in ileum (Fig. 7G).

In summary, at the start of the active/feeding period we observed a strongly increased dephosphorylation of S274 and a trend towards increased phosphorylation of S297 in the small intestine of WT mice. Taken together, based on the findings obtained with (de)phosphorylation-mimicking mutants in the *Xenopus laevis* oocyte expression system, these results suggest that in anticipation of the upcoming feeding period intestinal mLAT4 function is upregulated by changes in its phosphorylation, ensuring a higher amino acid uptake capacity.

Discussion

The aim of our study was to determine the possible role of phosphorylation of basolateral amino acid transporter LAT4 on serines S274, S278 and S297 in the regulation of intestinal amino acid absorption. Experiments with mutant hLAT4 constructs mimicking various phosphorylation states in *Xenopus laevis* oocytes indicated that the non-phosphorylated state of S274 favours the mature, terminally glycosylated form and surface expression of hLAT4, and increases its transport function. In contrast, the non-phosphorylated state of S297 led to almost non-functional hLAT4. *In vivo* investigations with food-entrained mice revealed that anticipation of food intake does not affect mLAT4 mRNA and protein expression or mLAT4 subcellular localization in the small intestine. However, using our new phosphosite-specific antibodies we observed a decreased phosphorylation of mLAT4 S274 and a trend towards increased pS297 levels in the small intestine of these mice. This suggests, based on our results obtained in *Xenopus laevis* oocytes, that the function of LAT4 is upregulated by food intake anticipation. Thus, the basolateral amino acid uniporter LAT4 appears to be regulated by phosphorylation and this regulatory mechanism is used in the context of diurnal food entrainment.

The expression of phosphorylation site mutant hLAT4 in *Xenopus laevis* oocytes suggests possible regulatory roles

The results of our experiments using (de)phosphorylation-mimicking mutant hLAT4 constructs expressed

in *Xenopus laevis* oocytes allow us to formulate some hypotheses concerning the role of the corresponding post-translational modifications for the expression and function of the basolateral essential amino acid uniporter LAT4 that might also apply *in vivo*.

There might be several reasons why the phosphorylation-mimicking glutamate mutations of the tested serine residues had only relatively small, transport-decreasing effects (Fig. 1B and D, Table 2). The first possibility is that the engineered glutamate (E) residue does not efficiently mimic phosphorylation at sites that are already largely phosphorylated on WT hLAT4 expressed in *Xenopus* oocytes. This could, for instance, have been the case for pS297, which was strongly detected with anti-pS297 antibody on the terminally glycosylated form of WT hLAT4 expressed in *Xenopus* oocytes (Fig. 3). However, its replacement with glutamate did not support the active function of hLAT4 at the cell surface (Fig. 1B, Table 2) to the same extent. Yet, glutamate mutants have been successfully used to mimic phosphorylation before (Maciejewski *et al.* 1995; Szabo *et al.* 1997; Davies *et al.* 2002). Therefore, the second possibility is that glutamate mutations efficiently mimic the phosphorylation at sites that are not strongly phosphorylated in WT hLAT4 expressed in *Xenopus* oocytes, and the phosphorylation of which leads to a decrease in transport function. Such a scenario could apply to terminally glycosylated WT hLAT4, which seems to contain proportionally less pS274 than the core-glycosylated form (Fig. 3). In this case, the phosphorylation-mimicking glutamate mutation S274E would lead to a decrease in the hLAT4 transport function at the cell surface, as was also observed experimentally (Fig. 1B, Table 2).

In contrast to the rather uniform transport-decreasing effect of the phosphorylation-mimicking glutamate mutations, non-phosphorylated state-mimicking alanine mutations caused stronger alterations in hLAT4 function that were clearly site-specific (Figs 1A and C and 2C–F, Table 2). Dephosphorylation-mimicking alanine mutations of both S274 and S297 led similarly to a strong decrease in core-glycosylated and intracellular hLAT4 expression in *Xenopus* oocytes (Figs 1E, 2C and F, and 3). This observation suggests that continuous phosphorylation of S274 and/or of S297 tends to retain hLAT4 in an immature intracellular state and that at least a transient dephosphorylation of hLAT4 is required to allow its maturation along the secretory pathway. Concerning the transport function, S274A provoked a substantial increase in hLAT4 apparent affinity and thus of its transport activity at physiological amino acid concentrations (Fig. 1A, Table 2). In contrast, S297A had an opposite impact on hLAT4 function, by strongly decreasing its transport rate (Fig. 1A, Table 2), an observation already reported previously by Bodoy

et al. (2005). This reproducible observation suggests that without phosphorylation on S297, hLAT4 is hardly active at the cell surface.

In our studies using hLAT4-expressing MDCK cells (data not shown), WT mouse kidney (data not shown) and small intestine (Figs 4B and 6C), essentially only terminally glycosylated mLAT4 has been detected, as even the low molecular mass fragments still contain glycosylation (data not shown). In the small intestine, according to immunofluorescence images, mLAT4 localized to a large extent on or very close to the basolateral plasma membrane (Fig. 4C), and part of this glycosylated mLAT4 appeared on Western blots as proteolytic fragments (Fig. 5). These observations support the hypothesis that LAT4 needs to be terminally glycosylated to reach its localization on the plasma membrane and to contribute to transepithelial amino acid transport. Interestingly, our observations also suggest that the terminally glycosylated form of hLAT4 is phosphorylated at either S274 or S297 (Fig. 3). We can thus speculate that phosphorylation on S297 with simultaneous dephosphorylation of S274 could contribute to the stabilization of mature LAT4, its localization at the plasma membrane and increased apparent affinity, leading to an increased transport function as observed in the *Xenopus* oocyte expression system. On the other hand, dephosphorylation of S297 would be a major signal leading to a decrease in LAT4 function and overall expression level. However, some of this inactivated LAT4 may still be retained at the plasma membrane due to its phosphorylation at the level of S274.

Interestingly, we did not observe synergistic or additive effects of S274 and S278 double mutants on the hLAT4 uptake capacity and kinetic parameters (Fig. 1C and D, Table 2). Nonetheless, alanine mutation of S278 led to proportionally increased phosphorylation of S274 on terminally-glycosylated hLAT4, compared to WT (Fig. 3). Therefore, we speculate that in WT LAT4 these two sites might often display opposite phosphorylation states and/or could be linked in specific signalling pathways. For instance, it has been shown that S274 needs to be phosphorylated in order for S278 to fit the MAPKKK kinase motif (Christensen *et al.* 2010). Moreover, all kinase recognition motifs (MAPKAPK2, casein kinase II, GSK3 kinase) proposed for S278 by PhosphoMotif Finder, an online tool from the Human Protein Reference Database, also require pS at position 274 (Amanchy *et al.* 2007) (http://www.hprd.org/PhosphoMotif_finder). Various types of cross-talk between phosphorylation sites analogous to our observations have also been described for other transporters, for example, the apical Na⁺/H⁺ exchanger where simultaneous phosphorylation on three sites has been shown to regulate its function (Chen *et al.* 2015).

LAT4 proteolysis in the small intestine of mice

In the small intestine of mice, we detected multiple proteolytic bands of mLAT4 (Figs 4B, 5, 6C; ~48 kDa, 42 kDa, 38 kDa) that have not been reported before. Unpublished data from our group have shown that such proteolytic bands are not present in the total or membrane lysate preparations from mouse kidneys (data not shown) and WT hLAT4-expressing *Xenopus laevis* oocytes (Fig. 1E) or MDCK cells (data not shown). Gastrointestinal tract is a major site for protease action (Antalis *et al.* 2007), thus detection of mLAT4 proteolysis in the small intestine is not surprising. However, the recurrence of fragments with the same molecular mass in multiple intestinal tissue preparations hinted at cleavage of specific peptide bonds. Based on the observed fragment sizes (Fig. 5), LAT4 appears to be cleaved in the large intracellular loop close to the investigated phosphorylation sites. The same loop also contains two potential LAT4 ubiquitylation sites in positions K260 and K283 that have been detected in human and murine tissues (Kim *et al.* 2011; Wagner *et al.* 2012; Mertins *et al.* 2013). Furthermore, Gene Harmonizome software also predicts LAT4 interaction with ubiquitin C (Rouillard *et al.* 2016) (<http://amp.pharm.mssm.edu/Harmonizome>). Ubiquitination of some nutrient transporters has been shown to lead to their internalization and subsequent proteolysis within the lysosome (Horak, 2003). It has also been shown that such ubiquitination-induced internalization and proteolysis can require previous phosphorylation for substrate recognition (Nguyen *et al.* 2013). Thus, we speculate that ubiquitination might play a role in intestinal LAT4 internalization and degradation, presumably in relation with its phosphorylation. However, we did not observe any meaningful differences in proteolytic band patterns or intensity between our experimental groups.

Food entrainment provokes diurnal LAT4 phosphorylation rhythm suggesting regulation of its transport function

Time restricted feeding (TRF) is a powerful cue to entrain peripheral oscillators and to reset the diurnal rhythms (Damiola *et al.* 2000; Konturek *et al.* 2011). It can lead to the upregulation of multiple macronutrient transporters at the time of expected food intake (Hussain & Pan, 2015). For the intestinal peptide (PEPT1) and the sodium-dependent glucose (SGLT1) transporters, this upregulation has been shown to be mediated by an increase in their protein and/or mRNA expression levels (Pan *et al.* 2002, 2004; Saito *et al.* 2008; Hussain & Pan, 2015). In our study we entrained mice with time-restricted feeding from ZT12 to ZT20 (first 8 h of the dark, active period) and did not observe significant changes in mLAT4

overall expression or localization in the small intestine between the anticipated feeding time (ZT12) and the postprandial phase (ZT0) (Fig. 4). However, we observed that food anticipation led to an overall strong decrease in S274 phosphorylation and a marginal increase in S297 phosphorylation levels (Fig. 7). Considering that the effects observed with hLAT4 mutants expressed in *Xenopus laevis* oocytes can be extrapolated to murine intestinal LAT4, this would indicate that LAT4 function and stability are increased at the anticipated feeding time, suggesting a diurnal regulatory response to food entrainment.

Phosphorylation is one of the least energy demanding functional switch processes in the cell, making it a very attractive regulatory mechanism. It is known to be used for the regulation of most circadian clock proteins (Schacter *et al.* 1984; Reischl & Kramer, 2011; Pacha & Sumova, 2013). The importance of phosphorylation in the context of circadian regulation was recently impressively supported by the result of a large-scale phosphoproteomics study that investigated more than 20,000 phosphosites on different proteins in mouse liver. It revealed that approximately 25% of the tested phosphosites show diurnal oscillations in phosphorylation levels, some of which also locate in SLCs, including the amino acid transporters CAT2 (SLC7A2), SNAT4 and SNAT9 (SLC38A4/A9). Importantly, the proportion of phosphorylation sites with circadian oscillations and the amplitude of their changes was shown to be much larger than that of transcripts and proteins, of which only about 10% display a circadian oscillation (Robles *et al.* 2017). These results indicate that phosphorylation might play a greater role in circadian regulation than previously thought, even though to our knowledge phosphorylation has not yet been directly linked to diurnal regulation of intestinal nutrient transporters.

Our study has revealed the circadian phosphorylation of the basolateral small intestine amino acid uniporter LAT4 and suggests, based on functional investigations performed in the *Xenopus laevis* oocytes, that this phosphorylation leads to an increased absorption capacity at the expected feeding time. We propose that phosphorylation plays an important, if not the main role in diurnal regulation of basolateral amino acid transporter LAT4. However, an important limitation of our study is the fact that only two time points ZT0 and ZT12 were investigated. As we lack a continuous view of LAT4 phosphorylation, mRNA and protein expression changes over 24 h, we cannot exclude that such changes might occur at other time points. Therefore, in follow-up studies it would be interesting to investigate LAT4 regulation at additional time points, the effect of the dietary protein content and the role of cellular regulatory networks in the control of food-entrained circadian phosphorylation changes.

Of course, linking phosphorylation changes in LAT4 with its amino acid absorptive function *in vivo* could represent a major strengthening of our food expectation hypothesis. However, this does not appear to be feasible yet, since we are not able to distinguish *in vivo* between the functional impact of LAT4 regulation and that of other amino acid transporters or, alternatively, to phosphorylate LAT4 independently of other proteins.

An intriguing observation made in this study was the localization pattern of S274 phosphorylation on small intestinal villi at the time of food expectation: at ZT12 it distributed in relatively large patches of cells often covering the top and/or the bottom of villi or, alternatively, their middle part. This localization pattern was variable along the duodenum and the jejunum (Fig. 7B and E) and also between neighbouring villi, whereas S274 phosphorylation was nearly absent from ileum (Fig. 7G). We speculate that LAT4 phosphorylation and thus function are regulated as an adaptation to the expected amino acid availability and correspond to a location-specific optimization of the transport processes along the intestine (Moran, 2016). But this does not explain the patchy pattern of the phosphorylation distribution. Looking at the literature, we were not able to find any distribution pattern of proteins or phosphorylation along villi that resembled our observation. We are also not aware of metabolic processes with patch-specific activity in villus. Thus, we cannot yet provide a good explanation for this surprising distribution pattern of mLAT4 S274 phosphorylation.

Taken together, our results have shown that the basolateral amino acid uniporter LAT4 is subject to a circadian regulation by phosphorylation in the mouse small intestine, and this novel regulatory mechanism is suggested to play an important role in the diurnal regulation of amino acid absorption.

References

- Albrecht U (2012). Timing to perfection: The biology of central and peripheral circadian clocks. *Neuron* **74**, 246–260.
- Amanchy R, Periaswamy B, Mathivanan S, Reddy R, Tattikota SG & Pandey A (2007). A compendium of curated phosphorylation-based substrate and binding motifs. *Nat Biotechnol* **25**, 285–286.
- Antalis TM, Shea-Donohue T, Vogel SN, Sears C & Fasano A (2007). Mechanisms of disease: protease functions in intestinal mucosal pathobiology. *Nat Clin Pract Gastroenterol Hepatol* **4**, 393–402.
- Balakrishnan A, Tavakkolizadeh A & Rhoads DB (2012). Circadian clock genes and implications for intestinal nutrient uptake. *J Nutr Biochem* **23**, 417–422.
- Bedet C, Isambert MF, Henry JP & Gasnier B (2000). Constitutive phosphorylation of the vesicular inhibitory amino acid transporter in rat central nervous system. *J Neurochem* **75**, 1654–1663.
- Bodoy S, Martin L, Zorzano A, Palacin M, Estevez R & Bertran J (2005). Identification of LAT4, a novel amino acid transporter with system L activity. *J Biol Chem* **280**, 12002–12011.
- Bohmer C, Broer A, Munzinger M, Kowalczyk S, Rasko JEJ, Lang F & Broer S (2005). Characterization of mouse amino acid transporter B⁰AT1 (Slc6a19). *Biochem J* **389**, 745–751.
- Broer S (2008). Amino acid transport across mammalian intestinal and renal epithelia. *Physiol Rev* **88**, 249–286.
- Broer S & Broer A (2017). Amino acid homeostasis and signalling in mammalian cells and organisms. *Biochem J* **474**, 1935–1963.
- Chen T, Kocinsky HS, Cha B, Murtazina R, Yang J, Tse CM, Singh V, Cole R, Aronson PS, de Jonge H, Sarker R & Donowitz M (2015). Cyclic GMP Kinase II (cGKII) inhibits NHE3 by altering its trafficking and phosphorylating NHE3 at three required sites. *J Biol Chem* **290**, 1952–1965.
- Christensen GL, Kelstrup CD, Lyngso C, Sarwar U, Bogebo R, Sheikh SP, Gammeltoft S, Olsen JV & Hansen JL (2010). Quantitative phosphoproteomics dissection of seven-transmembrane receptor signalling using full and biased agonists. *Mol Cell Proteomics* **9**, 1540–1553.
- Damiola F, Minh NL, Preitner N, Kornmann B, Fleury-Olela F & Schibler U (2000). Restricted feeding uncouples circadian oscillators in peripheral tissues from the central pacemaker in the suprachiasmatic nucleus. *Genes Dev* **14**, 2950–2961.
- Dave MH, Schulz N, Zevic M, Wagner CA & Verrey F (2004). Expression of heteromeric amino acid transporters along the murine intestine. *J Physiol* **558**, 597–610.
- Davies H, Bignell GR, Cox C, Stephens P, Edkins S, Clegg S, Teague J, Woffendin H, Garnett MJ, Bottomley W, Davis N, Dicks E, Ewing R, Floyd Y, Gray K, Hall S, Hawes R, Hughes J, Kosmidou V, Menzies A, Mould C, Parker A, Stevens C, Watt S, Hooper S, Wilson R, Jayatilake H, Gusterson BA, Cooper C, Shipley J, Hargrave D, Pritchard-Jones K, Maitland N, Chenevix-Trench G, Riggins GJ, Bigner DD, Palmieri G, Cossu A, Flanagan A, Nicholson A, Ho JWC, Leung SY, Yuen ST, Weber BL, Seigler HF, Darrow TL, Paterson H, Marais R, Marshall CJ, Wooster R, Stratton M & Futreal PA (2002). Mutations of the BRAF gene in human cancer. *Nature* **421**, 949–954.
- Deribe YL, Pawson T & Dikic T (2010). Posttranslational modifications in signal integration. *Nat Struct Mol Biol* **17**, 666–672.
- Gazzola RF, Sala R, Bussolati O, Visigalli R, Dall'Asta V, Ganapathy V & Gazzola GC (2001). The adaptive regulation of amino acid transport system A is associated to changes in ATA2 expression. *FEBS Letters* **490**, 11–14.
- Gilbert ER, Wong EA & Webb KE Jr (2008). Broad-invited review: Peptide absorption and utilization: Implications for animal nutrition and health. *J Anim Sci* **86**, 2135–2155.
- Gonzalez MI, Kazanietz MG & Robinson MB (2002). Regulation of the neuronal glutamate transporter excitatory amino acid carrier-1 (EAAC1) by different protein kinase C subtypes. *Mol Pharmacol* **62**, 901–910.
- Guetg A, Mariotta L, Bock L, Herzog B, Fingerhut R, Camargo SMR & Verrey F (2015). Essential amino acid transporter Lat4 (Slc43a2) is required for mouse development. *J Physiol* **593**, 1273–1289.

- Havel JP (2001). Peripheral signals conveying metabolic information to the brain: short-term and long-term regulation of food intake and energy homeostasis. *Exp Biol Med* **226**, 963–977.
- Hediger AM, Romero MF, Peng J, Rolfs A, Takanaga H & Bruford AE (2004). The ABCs of solute carriers: physiological, pathological and therapeutic implication of human membrane transport proteins. *Pflugers Arch* **447**, 465–468.
- Horak J (2003). The role of ubiquitin in down-regulation and intracellular sorting of membrane proteins: insights from yeast. *BBA Biomembranes* **1614**, 139–155.
- Hornbeck PV, Zhang B, Murray B, Kornhouser JM, Latham V & Skrzypek E (2015). PhosphoSitePlus, 2014: mutations, PTMs and recalibrations. *Nucleic Acids Res* **43**, D512–D520.
- Hundal HS & Taylor PM (2009). Amino acid transporters: gate keepers of nutrient exchange and regulators of nutrient signalling. *Am J Physiol Endocrinol Metab* **296**, E603–E613.
- Hussain MM & Pan X (2015). Circadian regulation of macronutrient absorption. *J Biol Rhythms* **30**, 459–469.
- Jando J, Camargo SMR, Herzog B & Verrey F (2017). Expression and regulation of the neutral amino acid transporter B⁰AT1 in rat small intestine. *PLoS One* **12**, e0184845.
- Karve TM & Cheema AK (2011). Small changes huge impact: The role of protein posttranslational modifications in cellular homeostasis and disease. *J Amino Acids* **2011**, 207691.
- Kim W, Bennet EJ, Huttlin EL, Guo A, Li J, Possemato A, Sowa ME, Rad R, Rush J, Comb MJ, Harper JW & Gygi SP (2011). Systematic and quantitative assessment of the ubiquitin-modified proteome. *Mol Cell* **44**, 325–340.
- Konturek PC, Brzozowski T & Konturek SJ (2011). Gut clock: Implication of circadian rhythms in the gastrointestinal tract. *J Physiol Pharmacol* **62**, 139–150.
- Liu T, Konkalmatt PR, Yang Y & Jose PA (2016). Gastrin decreases Na⁺,K⁺-ATPase activity via PI 3-kinase and PKC-dependent pathway in human renal proximal tubule cells. *Am J Physiol Endocrinol Metab* **310**, E565–E571.
- McGivan JD & Pastor-Anglada M (1994). Regulatory and molecular aspects of mammalian amino acid transport. *J Biochem* **299**, 321–334.
- Maciejewski PM, Peterson FC, Anderson PJ & Brooks CL (1995). Mutation of serine 90 to glutamic acid mimics phosphorylation of bovine prolactin. *J Biochem Mol Bio* **270**, 27661–27665.
- Makrides V, Camargo SMR & Verrey F (2014). Transport of amino acids in the kidney. *Compr Physiol* **4**, 367–403.
- Mariotta L, Ramadan T, Singer D, Guetg A, Herzog B, Stoeger C, Palacin M, Lahoutte T, Camargo SMR & Verrey F (2012). T-type amino acid transporter TAT1 (Slc16a10) is essential for extracellular aromatic amino acid homeostasis control. *J Physiol* **590**, 6413–6424.
- Meier C, Ristic Z, Klausner S & Verrey F (2002). Activation of system L heterodimeric amino acid exchangers by intracellular substrates. *EMBO* **21**, 580–589.
- Mertins P, Qiao JW, Patel J, Udeshi ND, Clauser KR, Mani DR, Burgess MW, Gillette MA, Jaffe JD & Carr SA (2013). Integrated proteomic analysis of post-translational modifications by serial enrichment. *Nat Methods* **10**, 634–637.
- Mizoguchi K, Cha SH, Chairoungdua A, Kim DK, Shigeta Y, Matsuo H, Fukushima J, Awa Y, Akakura K, Goya T, Ito H, Endou H & Kanai Y (2001). Human cystinuria-related transporter: Localization and functional characterization. *Kidney Int* **59**, 1821–1833.
- Mohawk JA, Green CB & Takahashi JS (2012). Central and peripheral circadian clocks in mammals. *Annu Rev Neurosci* **35**, 445–462.
- Moolenbeek C & Ruitenberg EJ (1981). The “Swiss roll”: a simple technique for histological studies of the rodent intestine. *Lab Anim* **15**, 57–59.
- Moran Jr ET (2016). Gastric digestion of protein through pancreatic action optimizes intestinal forms for absorption, mucin formation and villus integrity. *Anim Feed Sci Technol* **221**, 284–303.
- Nassl AM, Rubio-Aliaga I, Fenselau H, Marth MK, Kottra G & Daniel H (2011). Amino acid absorption and homeostasis in mice lacking the intestinal peptide transporter PEPT1. *Am J Physiol Gastrointest Liver Physiol* **301**, G128–G137.
- Nguyen LK, Kolch W & Kholodenko BN (2013). When ubiquitination meets phosphorylation: a systems biology perspective of EGFR/MAPK signalling. *Cell Commun Signal* **11**, 52.
- Pacha J & Sumova A (2013). Circadian regulation of epithelial functions in the intestine. *Acta Physiol (Oxf)* **208**, 11–24.
- Palacin M, Estevez R, Bertran J & Zorzano A (1998). Molecular biology of mammalian plasma membrane amino acid transporters. *Physiol Rev* **78**, 969–1054.
- Pan X, Terada T, Irie M, Saito H & Inui K (2002). Diurnal rhythm of H⁺ peptide co-transporter in rat small intestine. *Am J Physiol Gastrointest Liver Physiol* **283**, G57–G64.
- Pan X, Terada T, Okuda M & Inui K (2004). The diurnal rhythm of the intestinal transporters SGLT1 and PEPT1 is regulated by the feeding conditions in rats. *J Nutr* **134**, 2211–2215.
- Pendergast JS, Nakamura W, Friday RC, Hatanaka F, Takumi T & Yamazaki S (2009). Robust food anticipatory activity in BMAL1-deficient mice. *PLoS One* **4**, e4860.
- Poncet N & Taylor PM (2013). The role of amino acid transporters in nutrition. *Curr Opin Clin Nutr Metab Care* **16**, 57–65.
- Ramadan T, Camargo SMR, Herzog B, Bordin M, Pos KM & Verrey F (2007). Recycling of aromatic amino acids via TAT1 allows efflux of neutral amino acids via LAT2-4F2hc exchanger. *Pflugers Arch* **454**, 507–516.
- Ramadan T, Camargo SMR, Summa V, Hunziker P, Chesnov S, Pos KM & Verrey F (2006). Basolateral aromatic amino acid transporter TAT1 (Slc16a10) functions as an efflux pathway. *J Cell Physiol* **206**, 771–779.
- Reischl S & Kramer A (2011). Kinases and phosphatases in the mammalian circadian clock. *FEBS Lett* **585**, 1393–1399.
- Robles MS, Humphrey SJ & Mann M (2017). Phosphorylation is a central mechanism for circadian control of metabolism and physiology. *Cell Metab* **25**, 118–127.
- Rossier G, Meier C, Bauch C, Summa V, Sordat B, Verrey F & Kuhn LC (1999). LAT2, a new basolateral

- 4F2hc/CD98-associated amino acid transporter of kidney and intestine. *J Biol Chem* **274**, 34948–34954.
- Rouillard AD, Gunderson GW, Fernandez NF, Wang Z, Monteiro CD, McDermott MG & Ma'ayan A (2016). The harmonizome: a collection of processed datasets gathered to serve and mine knowledge about genes and proteins. *Database (Oxford)* **2016**, baw100.
- Saito H, Terada T, Shimakura J, Katsura T & Inui K (2008). Regulatory mechanism governing the diurnal rhythm of intestinal H⁺/peptide cotransporter 1 (PEPT1). *Am J Physiol Gastrointest Liver Physiol* **295**, G395–G402.
- Samluk L, Czeredys M, Skowronek K & Nalecz KA (2012). Protein kinase C regulates amino acid transporter ATB⁰⁺. *Biochem Biophys Res Commun* **422**, 64–49.
- Schachter E, Chock BP & Stadtman ER (1984). Energy consumption in a cyclic phosphorylation/dephosphorylation cascade. *J Biol Chem* **259**, 12260–12264.
- Schibler U, Gotic I, Saini C, Gos P, Curie T, Emmenegger Y, Sinturel F, Gosselin P, Gerber A, Fleury-Olela F, Rando G, Demarque M & Franken P (2015). Clock-talk: Interactions between central and peripheral circadian oscillators in mammals. *Cold Spring Harb Symp Quant Biol* **80**, 223–232.
- Schneider CA, Rasband WS & Eliceiri KW (2012). NIH Image to ImageJ: 25 years of image analysis. *Nat Methods* **9**, 671–675.
- Silk DBA, Grimble GK & Rees RG (1985). Protein digestion and amino acid and peptide absorption. *Proc Nutr Soc* **44**, 63–72.
- Stephan FK, Swann JM & Sisk CL (1979). Entrainment of circadian rhythms by feeding schedules in rats with suprachiasmatic lesions. *Behav and Neural Biol* **25**, 545–554.
- Szabo K, Bakos E, Welker E, Muller M, Goodfellow HR, Higgins CF, Varadi A & Sarkadi B (1997). Phosphorylation site mutations in the human multidrug transporter to modulate its drug-stimulated ATPase activity. *J Biol Chem* **272**, 23165–23171.
- Tanaka K, Yamamoto A & Fujita T (2005). Functional expression and adaptive regulation of Na-dependent neutral amino acid transporter SNAT2/ATA2 in normal human astrocytes under amino acid starved condition. *Neurosci Lett* **378**, 70–75.
- Taslimifar M, Oparija L, Verrey F, Kurtcuoglu V, Olgac U & Makrides V (2017). Quantifying the relative contributions of different solute carriers to aggregate substrate transport. *Sci Rep* **7**, 40628.
- Venne AS, Kollipara L & Zahedi RP (2014). The next level of complexity: Crosstalk of posttranslational modifications. *Proteomics* **14**, 513–524.
- Verrey F (2003). System L: heteromeric exchangers of large, neutral amino acids involved in directional transport. *Pflugers Arch* **445**, 529–533.
- Vilches C, Boiadjieva-Knopfel E, Boday S, Camargo S, Lopez de Heredia M, Prat E, Ormazabal A, Artuch R, Zorzano A, Verrey F, Nunes V & Palacin M (2018). Cooperation of antiporter LAT2/CD98hc with uniporter TAT1 for renal reabsorption of neutral amino acids. *J Am Soc Nephrol* **29**, 1624–1635.
- Wagner SA, Beli P, Weinert BT, Scholz C, Kelstrup CD, Young C, Nielsen ML, Olsen JV, Brakebusch C & Choudhary C (2012). Proteomic analysis reveals divergent ubiquitylation site patterns in murine tissues. *Mol Cell Proteomics* **11**, 1578–1585.
- Welsh DK, Takahashi JS & Kay SA (2010). Suprachiasmatic nucleus: Cell autonomy and network properties. *Annu Rev Physiol* **72**, 551–577.
- William HK & Diamond JM (1983). Adaptive regulation of sugar and amino acid transport by vertebrate intestine. *Am J Physiol Gastrointest Liver Physiol* **245**, G443–G462.
- Wu G (2016). Dietary protein intake and human health. *Food Funct* **7**, 1251–1265.
- Yi-lin L, Ke Z, Dan W, Xi-hong Z, Zheng R, Xin W & Yu-long Y (2017). Dynamic feeding low and high methionine diets affect the diurnal rhythm of amino acid transporters and clock related genes in jejunum of laying hens. *Biol Rhythm Res* **49**, 671–679. Available at: <http://doi.org/10.1080/09291016.2017.1395531>.

Additional information

Competing interests

The authors of this study confirm there are no competing interests.

Author contributions

All experiments were carried out at the University of Zurich in Zurich, Switzerland. L.O., A.R., N.P. and F.V. designed the study and necessary experiments. L.O., A.R. and N.P. carried out the experiments. L.O. and F.V. analysed and interpreted the data. L.O. and F.V. wrote and critically revised the manuscript. All authors approved the final version of the manuscript and agree to be held accountable for all aspects of this study. All persons qualifying for authorship are listed as such.

Funding

This study was supported by the Swiss National Science Foundation Grant No. 31_166430/1.

Acknowledgements

We would like to thank Eva Hänsenberger and Carlos Muñoz-Hernando for their help with oocyte harvesting from *Xenopus laevis* frogs, and Adriano Guetg and Ian Forster for their advice regarding radiolabelled substrate uptake experiments and LAT4 mutagenesis. We also thank Zurich Integrative Rodent Physiology Facility and the Zurich Center for Microscopy and Image analysis, especially Moritz Kirschmann, for their help and equipment.